

**STRENGTH PROPERTIES OF LATEX BASED
RUBBERIZED CONCRETE WITH 15 KG/M³
STEEL FIBER**

EMILY ENG LE YI

UNIVERSITI TUNKU ABDUL RAHMAN

**STRENGTH PROPERTIES OF LATEX BASED RUBBERIZED
CONCRETE WITH 15 KG/M³ STEEL FIBER**

EMILY ENG LE YI

**A project report submitted in partial fulfilment of the
requirements for the award of Bachelor of Civil
Engineering with Honours**

**Lee Kong Chian Faculty of Engineering and Science
Universiti Tunku Abdul Rahman**

May 2023

DECLARATION

I hereby declare that this project report is based on my original work except for citations and quotations which have been duly acknowledged. I also declare that it has not been previously and concurrently submitted for any other degree or award at UTAR or other institutions.

Signature :  _____

Name : EMILY ENG LE YI

ID No. : 1801586

Date : 10/5/2023

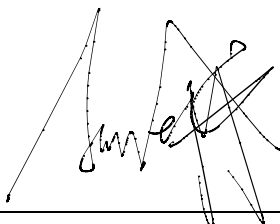
APPROVAL FOR SUBMISSION

I certify that this project report entitled “**STRENGTH PROPERTIES OF LATEX BASED RUBBERIZED CONCRETE WITH 15 KG/M³ STEEL FIBER**” was prepared by **EMILY ENG LE YI** has met the required standard for submission in partial fulfilment of the requirements for the award of Bachelor of Civil Engineering with Honours at Universiti Tunku Abdul Rahman.

Approved by,

Signature

:



Supervisor

:

IR DR LIM SIONG KANG

Date

:

16/5/2023

The copyright of this report belongs to the author under the terms of the copyright Act 1987 as qualified by Intellectual Property Policy of Universiti Tunku Abdul Rahman. Due acknowledgement shall always be made of the use of any material contained in, or derived from, this report.

© 2023, EMILY ENG LE YI. All right reserved.

ACKNOWLEDGEMENTS

I would like to express my sincere appreciation and gratitude to all those who have supported me in completing this project. First and foremost, I would like to express my gratitude to my research supervisor, Ir. Dr. Lim Siong Kang for his unwavering guidance, expertise, and encouragement throughout the entire process.

Besides, I would like to express my gratitude to all the lab staff in KBS01, KBS02 and KBS03. Without their assistance, this work would not have been possible.

In addition, I would also like to express heartfelt appreciation to my loving parents and friends for their constant love, support, and understanding.

ABSTRACT

Nowadays, the disposal of waste tires has led to serious environmental issues due to the rubber material being non-biodegradable. Hence, the way to reduce the number of waste tires is by converting waste tires into valuable and useful products and materials. Crumb rubber is one of the materials that can be added to concrete to form rubberized concrete. Rubberized concrete has better impact resistance, toughness and ductility but possesses lower strength than regular concrete. The reduction in mechanical strength can be attributed to the weak interfacial transition zones between the crumb rubber and hardened cement paste. The use of steel fiber and SBR latex has the ability to make up for the strength loss caused by the incorporation of crumb rubber. In addition, it should be noted that concrete exhibits a deficiency in its ability to withstand tensile forces, thereby requiring the incorporation of steel fiber in order to enhance its tensile capacity. Thus, this study examines the impact of incorporating steel fiber into latex based rubberized concrete (LRC) on compressive, flexural and splitting tensile strengths, as well as impact resistance. The optimum mix proportion of trial mix for both LRC and Latex based rubberized concrete with 15 kg/m^3 steel fiber (LRC-15 % SF) that had achieved at least 55 MPa of 28 days compressive strength was selected to test for the compressive, flexural and splitting tensile strengths, as well as impact resistance. Experimental results showed that steel fiber incorporation induced an enhancement in the strength properties of LRC. The experimental results indicate that the LRC-15 % SF with a W/C ratio of 0.28 exhibited superior performance compared to the control mixture with the same W/C ratio. Specifically, the LRC-15 % SF demonstrated a 3.18 % increase in compressive strength, a 10.70 % increase in splitting tensile strength, and a 17.94 % increase in flexural strength after 56 days of curing. Besides, the LRC-15 % SF showed higher impact resistance by 46.27 % and 14.71 % in the 400 mm and 200 mm span length impact test at 56 days, respectively. In short, the inclusion of steel fiber enhanced the performance of the concrete structure.

TABLE OF CONTENTS

DECLARATION		i
APPROVAL FOR SUBMISSION		ii
ACKNOWLEDGEMENTS		iv
ABSTRACT		v
TABLE OF CONTENTS		vi
LIST OF TABLES		x
LIST OF FIGURES		xi
LIST OF SYMBOLS / ABBREVIATIONS		xiv
LIST OF APPENDICES		xvi
CHAPTER		
1	INTRODUCTION	1
1.1	General Introduction	1
1.2	Importance of the Study	2
1.3	Problem Statement	3
1.4	Aim and Objectives	4
1.5	Scope and Limitation of the Study	4
1.6	Contribution of the Study	5
1.7	Outline of the Report	5
2	LITERATURE REVIEW	7
2.1	Introduction to Rubberized Concrete	7
2.1.1	Advantages of Rubberized Concrete	8
2.1.2	Application of Rubberized Concrete	8
2.2	Crumb Rubber	9
2.2.1	Processing of Crumb Rubber	10
2.2.2	Properties of Crumb Rubber	11
2.3	Properties of Rubberized Concrete	11
2.3.1	Workability	12
2.3.2	Bulk Density	12

2.3.3	Compressive Strength	13
2.3.4	Flexural Strength	13
2.3.5	Splitting Tensile Strength	13
2.3.6	Impact Resistance	14
2.4	Interface Transition Zone	14
2.5	Styrene-Butadiene Latex	15
2.5.1	Properties of Latex Modified Concrete	16
2.6	Latex Based Rubberized Concrete	17
2.6.1	Properties of Latex Based Rubberized Concrete	18
2.7	Steel Fiber	19
2.7.1	Properties of Steel Fiber Reinforcement Rubberized Concrete	21
2.8	Ordinary Portland Cement	23
2.9	Aggregate	24
2.10	Superplasticizer	24
2.11	Silica Fume	25
2.12	Summary	26
3	METHODOLOGY AND WORK PLAN	28
3.1	Introduction	28
3.2	Flow Chart of the Study	29
3.3	Raw Material	30
3.3.1	Ordinary Portland Cement (OPC)	30
3.3.2	Coarse Aggregate, Fine Aggregate and Crumb Rubber	33
3.3.3	Water and Superplasticizer	38
3.3.4	Styrene-Butadiene (SBR) Latex	39
3.3.5	Silica Fume	40
3.3.6	Steel Fiber	41
3.4	Concrete Mould	43
3.5	Trial Mix	46
3.6	Mixing Procedure	47
3.7	Fresh State Properties Test	48
3.7.1	Slump Test	49

	3.7.2 Compacting Factor Test	50
	3.8 Casting Procedure	51
	3.9 Curing	52
	3.10 Hardened State Properties Test	54
	3.10.1 Compression Test (BS EN 12390-3)	55
	3.10.2 Splitting Tensile Test (BS EN 12390-6)	56
	3.10.3 Flexural Test (BS EN 12390-5)	57
	3.10.4 Repeated Drop Weight Impact Test	58
	3.11 Scanning Electron Microscope and Energy Dispersive X-ray Analysis	59
	3.11.1 Scanning Electron Microscope (SEM)	60
	3.11.2 Energy Dispersive X-ray (EDX)	61
	3.12 Summary	62
4	TRIAL MIX	64
	4.1 Introduction	64
	4.2 Tensile Testing for Steel Fiber	64
	4.3 Control Mix	65
	4.3.1 Fresh Properties	66
	4.3.2 Density	67
	4.3.3 Compressive Strength	68
	4.4 Steel Fiber Mix	68
	4.4.1 Fresh Properties	69
	4.4.2 Density	70
	4.4.3 Compressive Strength	71
	4.5 Summary	71
5	RESULTS AND DISCUSSION	73
	5.1 Introduction	73
	5.2 Real Mix Proportions	73
	5.3 Fresh Properties	75
	5.4 Density	75
	5.5 Hardened Properties	76
	5.5.1 Compressive Strength	76
	5.5.2 Splitting Tensile Strength	78
	5.5.3 Flexural Strength	80

5.5.4	Impact Resistance	83
5.6	SEM Morphologies	86
5.7	Elemental Compositions (EDX analysis)	87
5.8	Effect of Various Steel Fiber Content on Hardened Properties	89
5.8.1	Compressive Strength	89
5.8.2	Splitting Tensile Strength	90
5.8.3	Flexural Strength	91
5.8.4	Impact Resistance	92
5.9	Summary	94
6	CONCLUSION AND RECOMMENDATIONS	95
6.1	Conclusion	95
6.2	Recommendations for future work	96
	REFERENCES	97
	APPENDICES	106

LIST OF TABLES

Table 2.1:	Typical Contents of Automobile Tires (Li, et al., 2014).	10
Table 2.2:	Contents of OPC (Marchment, et al., 2019).	23
Table 3.1:	Properties of YTL Orang Kuat, CEM I Branded OPC (YTL Cement, 2022).	31
Table 3.2:	Typical Chemical Composition of 52.5 N OPC (Type 1) (Kanadasan, et al., 2015).	32
Table 3.3:	Bogue Compound Composition of 52.5 N OPC (Type 1) (Kanadasan, et al., 2015).	32
Table 3.4:	Fineness Modulus of Coarse Aggregate, Fine Aggregate and Crumb Rubber.	38
Table 3.5:	Properties of Stahlcon Hooked-End Steel Fiber.	42
Table 3.6:	Summary of the Mould Used for Test.	45
Table 4.1:	Tensile Test Results for Steel Fiber.	65
Table 4.2:	Mix Proportions of Trial Mixes for LRC-CTR.	66
Table 4.3:	Mix Proportions of Trial Mixes for LRC-15 % SF.	69
Table 5.1:	Design Mix Proportions of LRC-CTR and LRC-15 % SF.	74
Table 5.2:	Experimental Result of Impact Resistance Test.	83
Table 5.3:	Weight and Atomic Weightage of Element Composition.	88

LIST OF FIGURES

Figure 2.1:	SEM Micrograph of ITZ With Magnification of 348× (Gupta, Chaundhary and Sharma, 2014).	15
Figure 2.2:	Silica Fume on the Rubber Particle (Xu, et al., 2020).	25
Figure 3.1:	Design Flow Chart.	29
Figure 3.2:	YTL Orang Kuat, CEM I Branded OPC.	30
Figure 3.3:	Sieving of OPC.	33
Figure 3.4:	Sieved OPC in an Air-Tight Container.	33
Figure 3.5:	Fine Aggregates Retained on the Receiving Pan.	34
Figure 3.6:	Coarse and Fine Aggregate Oven-Dried in the Oven.	35
Figure 3.7:	Crumb Rubbers.	36
Figure 3.8:	Set Up of Sieve Analysis Test.	37
Figure 3.9:	Finer in Mass Against Particle Size.	37
Figure 3.10:	BASF Superplasticizer.	39
Figure 3.11:	Styrene-Butadiene (SBR) Latex.	40
Figure 3.12:	Silica Fume.	41
Figure 3.13:	Stahlcon Hooked-End Steel Fiber HE 0.55/35.	42
Figure 3.14:	Preparation of Tensile Test.	43
Figure 3.15:	Cubic Mould.	44
Figure 3.16:	Cylindrical Mould.	44
Figure 3.17:	Prism Mould.	45
Figure 3.18:	The Mould Was Cleaned With Air Blower.	46
Figure 3.19:	A Thin Layer of Oil Was Coated on the Mould's Surface.	46
Figure 3.20:	Fine Aggregate Was Weighted.	48
Figure 3.21:	Crumb Rubber Coated With SBR Latex.	48

Figure 3.22: Concrete Mix Was Consolidated Using Tamping Rod.	50
Figure 3.23: Slumped Concrete.	50
Figure 3.24: Compacting Factor Test.	51
Figure 3.25: Fresh Concrete Was Transferred to the Prism Mould.	52
Figure 3.26: Water Curing for the Concrete Specimens.	53
Figure 3.27: Dimension Was Measured Using Vernier Calliper.	53
Figure 3.28: Concrete Was Weighted Using Weighing Machine.	54
Figure 3.29: Compressive Strength Test.	55
Figure 3.30: Splitting Tensile Strength Test.	57
Figure 3.31: Flexural Strength Test.	58
Figure 3.32: Repeated Drop Weight Impact Test.	59
Figure 3.33: Coating of Specimens in Sputter Coater Machine.	60
Figure 3.34: Specimens Were Placed in Vacuum Chamber.	61
Figure 3.35: Hitachi VP-SEM S-3700N.	62
Figure 4.1: Stress-Strain Curve for Steel Fiber.	65
Figure 4.2: Fresh Properties of Trial Mixes for LRC-CTR.	67
Figure 4.3: Density of Trial Mixes for LRC-CTR.	67
Figure 4.4: Compressive Strength of Trial Mixes for LRC-CTR.	68
Figure 4.5: Fresh Properties of Trial Mixes for LRC-15 % SF.	70
Figure 4.6: Density of Trial Mixes for LRC-15 % SF.	70
Figure 4.7: Compressive Strength of Trial Mixes for LRC-15 % SF.	71
Figure 5.1: Fresh Properties of LRC-CTR and LRC-15 % SF.	75
Figure 5.2: Density of LRC-CTR and LRC-15 % SF.	76
Figure 5.3: Compressive Strength of LRC-CTR and LRC-15 % SF.	78
Figure 5.4: Splitting Tensile Strength of LRC-CTR and LRC-15 % SF.	79

Figure 5.5:	Splitting Tensile/ Compressive Strength Ratio.	80
Figure 5.6:	Flexural Strength of LRC-CTR and LRC-15 % SF.	81
Figure 5.7:	Flexural / Compressive Strength Ratio.	81
Figure 5.8:	Flexural Failure of LRC-CTR.	82
Figure 5.9:	Flexural Failure of LRC-15 % SF.	82
Figure 5.10:	Impact Resistance of LRC-CTR and LRC-15 % SF.	84
Figure 5.11:	Fracture Pattern of LRC-CTR.	85
Figure 5.12:	Fracture Pattern of LRC-15 % SF.	85
Figure 5.13:	Fracture Pattern of LRC-CTR (200 mm).	86
Figure 5.14:	SEM Morphology (a) LRC-CTR (b) LRC-15 % SF.	87
Figure 5.15:	EDX Spectrum of LRC-15 % SF.	89
Figure 5.16:	Compressive Strength of Various Steel Fiber Design Mixes.	90
Figure 5.17:	Splitting Tensile Strength of Various Steel Fiber Design Mixes.	91
Figure 5.18:	Flexural Strength of Various Steel Fiber Design Mixes.	92
Figure 5.19:	Impact Resistance for 400 mm Span Length Impact Test.	93
Figure 5.20:	Impact Resistance for 200 mm Span Length Impact Test.	93

LIST OF SYMBOLS / ABBREVIATIONS

A_c	cross sectional area of specimen, m ²
B	width of specimen, mm
D	diameter, mm
d	depth of specimen, mm
E_{impact}	impact energy, kg·m ² /s ²
F	maximum load subjected the specimen, N
f_c	compressive strength, MPa
g	gravitational acceleration, m/s ²
h	height of drop weight, m
I	distance between supporting roller, mm
L	length of the specimen, mm
m	mass of drop weight, kg
N	number of drops to cause ultimate crack
P	maximum applied load, N
R	flexural strength, MPa
T	splitting tensile strength, MPa
v	volume of specimen, m ³
w	mass of specimen, kg
ρ	bulk hardened density, kg/m ³
ASTM	American Society for Testing and Materials
ACI	American Concrete Institute
Al	Aluminium
Al ₂ O ₃	Alumina
AFm	Monosulphate
BS EN	British Standards European Norm
C	Carbon
Ca	Calcium
CaO	Calcium Oxide/ Lime
CR	Crumb rubber
C ₂ S	Dicalcium silicate

C ₃ A	Tricalcium aluminate
C ₃ S	Tricalcium silicate
C ₄ AF	Tetracalcium aluminoferrite
CH	Portlandite
C-S-H	Calcium silicate hydrate
EDX	Energy Dispersive X-ray
Fe	Iron
Fe ₂ O ₃	Iron(III) Oxide/ Ferric Oxide/ Hematite
ITZ	Interfacial transition zone
K ₂ O	Potassium Oxide
LRC	Latex based rubberized concrete
LRC-15 % SF	Latex based rubberized concrete with 15 kg/m ³ steel fiber
Mg	Magnesium
MgO	Magnesium Oxide/ Magnesia/ Periclase
Mn ₂ O ₃	Manganese (III) Oxide
Na ₂ O	Sodium Oxide
O	Oxygen
OPC	Ordinary Portland Cement
RUC	Rubberized concrete
R-CM	Rubber-cement matrix
S	Sulphur
SBR	Styrene-butadiene latex
SEM	Scanning electron microscopy
SF	Steel fiber
SFRC	Steel fiber reinforced rubberized concrete
Si	Silicon
SiO ₂	Silicon Dioxide/ Silica
SO ₃	Sulphur Trioxide
SP	superplasticizers
P ₂ O ₅	Phosphorus Pentoxide
TiO ₂	Titanium Dioxide
W/C	Water to cement ratio

LIST OF APPENDICES

Appendix A-1:	Sieve Analysis of Coarse Aggregate.	106
Appendix A-2:	Sieve Analysis of Fine Aggregate.	107
Appendix A-3:	Sieve Analysis of Crumb Rubber.	107
Appendix A-4:	Compressive Strength for Trial Mixes of LRC-CTR.	108
Appendix A-5:	Compressive Strength for Trial Mixes of LRC-15 % SF.	108
Appendix A-6:	Compressive Strength of LRC-CTR and LRC-15 % SF.	108
Appendix A-7:	Splitting Tensile Strength of LRC-CTR and LRC-15 % SF.	108
Appendix A-8:	Flexural Strength of LRC-CTR and LRC-15%SF.	109

CHAPTER 1

INTRODUCTION

1.1 General Introduction

In the world of today, concrete play an important role in providing human with a rigid shelter or a workplace. Due to its strength and durability, concrete is used extensively in the building industry. It is a fundamental building element in this contemporary world. Even the quantity of concrete manufactured is ten times more than the production of steel (Tantawi, 2015). Concrete is an artificial stone manufactured by using cement, water, aggregates and suitable additives if required (Tantawi, 2015). Each variety of cement has its unique properties. Next, coarse and fine aggregates are the primary types of aggregates utilised in a concrete mixture. During the manufacturing process of concrete, the raw materials are mixed. The water will combine and react with cement to produce fresh cement paste. The fresh cement paste is then bound with aggregates and covers up the surface of aggregates. C_3S and C_2S react with water during the hydration process to generate the Calcium Silicate Hydrate (C-S-H) gel. Over a longer time, the cement paste will harden and form the rock-like mass known as concrete (Bordallo, Aldridge and Desmedt, 2006).

Rubber is an essential material that is widely employed in numerous industrial applications. For example, rubber can be used for various applications such as road construction, water barriers, geotechnical work, retaining walls, concrete mixtures, etc. Used rubber tires produce more waste as cars on the road rise. The disposal of rubber tires has an impact on the environment. The production of crumb rubber (CR) can resolve this environmental problem by utilising waste rubber. Crumb rubber is typically produced by reducing the used rubber tires into smaller particles (Xu, et al., 2020). Rubberized concrete (RUC) is a composite created by adding rubber crumbs to replace the aggregate in the concrete mix. Adding crumb rubber to concrete improves its performance in terms of toughness, ductility, fatigue and impact resistance (Hameed and Shashikala, 2016). However, the workability and mechanical strengths have been seen to decrease as rubber crumb content

increases (Bisht and Ramana, 2017). The strength reduction is due to the weak interfacial transition zone (ITZ) formed between cement paste and crumb rubber. Thus, styrene-butadiene (SBR) latex is utilised as a binding agent in the manufacturing of concrete to mitigate the strength loss resulting from the inclusion of crumb rubbers.

The performance of concrete is determined by the type of raw materials used and their amounts in the mixture. Different types of additives are added to fresh concrete to enhance the qualities of concrete. One of the negative features of concrete is its weakness in tension, which necessitates tensile reinforcement to enhance tensile strength. A composite known as fiber-reinforced concrete is created when short and uneven fibers are randomly dispersed in concrete. In cementitious composites, fibers are typically obtained from natural resources or made of steel, glass, and polymers (Chanh, 2015). Steel fiber (SF) is most often used to strengthen concrete. The inclusion of steel fibers can improve the strength and overall toughness of concrete. The steel fiber reinforced concrete exhibits superior strength compared to the ordinary reinforced concrete (Behbahani, Nematollahi and Farasatpour, 2011).

1.2 Importance of the Study

In recent years, the introduction of crumb rubber into concrete production has received a lot of attention due to the value placed on sustainable development. Using crumb rubber in the production of concrete helps maintain ecological balance and improves the economic value of concrete production. Furthermore, incorporating crumb rubber into concrete production improves the ductility and impact resistance of the concrete. However, when crumb rubber is added to concrete, the compressive, splitting, and flexural strengths are often reduced, according to a previous study on crumb rubber (Eisa, Elshazli and Nawar, 2020). Consequently, the rubber-modified concrete has been added to the schedule. SBR latex is utilised as a binding agent in this rubberized concrete production, potentially improving the strength. Besides, steel fiber is a material that has the potential to improve the performance of concrete. It improves the concrete's compressive and flexural. In short, the importance of this study is research on adding crumb rubber as part of aggregate replacement material to make the environment more sustainable. Furthermore, the

behaviour of the latex based rubberized concrete can be improved by introducing steel fiber reinforcement. Moreover, the importance of the study is to develop the optimum mix proportion and study the effect of combining crumb rubber, Styrene-Butadiene (SBR) latex and steel fiber on the impact resistance, compressive, splitting tensile and flexural strength.

1.3 Problem Statement

Waste tires have been classified as municipal solid waste. Therefore, tire disposal has become one of the environment's most critical issues. This is because the waste is not readily biodegradable even after a lengthy period at a landfill. Due to a significant depletion of waste disposal sites, numerous nations have prohibited the disposal of used waste tires in landfills. Even in some poor countries, residents do not consider the hazards to humans and the environment and use open fire and other improper ways to throw waste tires indiscriminately in valleys, roadsides, open areas and other places. One potential solution to this problem is reducing the waste tires to a more valuable product, crumbs rubber and adding it into the concrete to produce rubberized concrete. Rubberized concrete has been found to have good aesthetics and better impact resistance than regular concrete. However, it exhibits lower strength than regular concrete. The strength loss is mainly due to the weak ITZ between the crumb rubber and hardened cement matrix. Thus, adding SBR latex and steel fiber to the concrete mixture will allow the development of sufficient strength and make latex based rubberized concrete with steel fiber an ideal alternative construction material for flexible pavements.

1.4 Aim and Objectives

The main aim of this study is to produce latex based rubberized concrete (LRC) and latex based rubberized concrete with 15 kg/m³ steel fiber (LRC- 15 % SF).

The specific objectives as listed below:

- (i) To identify the optimum mix proportion for latex based rubberized concrete and latex based rubberized concrete with 15 kg/m³ steel fiber.
- (ii) To evaluate the fresh concrete properties in latex based rubberized concrete with 15 kg/m³ steel fiber, namely concrete workability and density.
- (iii) To evaluate the hardened concrete properties in terms of compressive strength, split tensile strength, flexural strength and impact resistance of latex based rubberized concrete with 15 kg/m³ steel fiber.

1.5 Scope and Limitation of the Study

There are numerous task scopes identified in this study. This study will investigate the impact of the incorporation between crumb rubber, SBR latex and steel fiber on the concrete's impact resistance, compressive, splitting tensile and flexural strengths. First of all, the desired mix proportion for the LRC-15 % SF will be obtained based on the trial mix result. Multiple trials mixes for LRC and LRC-15 % SF will be conducted. Then, all the sample specimens will be cast following the optimum mix proportion and cured for 7, 28 and 56 days. The raw material preparation and casting methods were conducted per BS EN and ASTM specifications. 150 mm × 150 mm × 150 mm of cubic specimens will be tested for compressive strength with a universal compression machine. The cylindrical specimen with a dimension of 100 mm in diameter and 200 mm in height will be used for the splitting tensile test. The prism specimen of 100 mm × 100 mm × 500 mm will be utilised to obtain the flexural strength in the flexural test. Besides, the prism specimen with 100 mm × 100 mm × 500 mm will also be utilised for the repeated drop weight impact test.

However, the concerning part of this study is the raw material preparation, especially for the crumb rubber. It is not easy to gather a group of

rubber aggregates that are all the same size. The rubber granules must be 1 to 4 mm in size. Besides, the unburned carbon black in the rubber composition may also be a limitation of this study. It will result in a weakening of the concrete.

1.6 Contribution of the Study

This study introduces an innovative approach by incorporating latex based rubber particles into the concrete mix along with steel fibers, which has not been extensively investigated in the existing literature. The combination of latex based rubberized concrete with steel fibers has the potential to improve the strength characteristics of concrete, making this study a significant contribution to the field of concrete technology. The study's results hold practical implications for the field of construction. The enhanced impact resistance derived from latex based rubberized concrete with steel fiber is of importance for railway sleepers, which are frequently exposed to significant impact loading during operation and tamping maintenance. The utilisation of latex based rubberized concrete with steel fiber in railway sleeper construction has significant potential for replacing conventional plain concrete. In addition, the incorporation of latex based rubber particles and steel fibers into the concrete mixture can potentially enhance sustainability by employing recycled rubber waste, mitigating environmental problems, and encouraging sustainable construction.

1.7 Outline of the Report

This report contains six chapters, which are the introduction, literature review, methodology, trial mixes results, results and discussion and lastly, conclusion and recommendations.

In chapter one, the background and importance of this study are generally explained. Then, the problems to be investigated relating to this topic are described to know why this study is important to be conducted. Besides, the aim and objective related directly and logically to the problem statement are stated. Furthermore, the scope and limitations of this study are mentioned clearly. Finally, at the end of this chapter, an outline of the report is presented.

Next, chapter two discusses the literature review on rubberized concrete, LRC and RUC with steel fiber reinforcement. Besides, the engineering properties and materials such as SBR latex, OPC, aggregates, superplasticizers and silica fume are discussed.

In chapter three, the material preparation, mixing procedure, casting procedure and testing procedure are described in detail.

Then, chapter four summarises the tensile testing for steel fiber, fresh properties and compressive strength of the trial mixes of LRC-CTR and LRC-15 % SF. Besides, the optimum mix proportion of LRC-CTR and LRC-15 % SF with a minimum compressive strength of 55 MPa at 28 days is discussed.

After that, chapter five compares LRC-CTR and LRC-15 % SF in terms of workability, density, compressive strength, splitting tensile strength, flexural strength and impact resistance. Besides, the surface microstructure morphologies and elemental compositions of LRC-CTR and LRC-15 % SF from the SEM-EDX analysis are discussed.

Lastly, chapter six provides a summary of the experimental findings obtained from varied tests. Additionally, recommendations are presented to enhance the comprehensiveness of future studies.

CHAPTER 2

LITERATURE REVIEW

2.1 Introduction to Rubberized Concrete

Concrete has been utilised as a construction material for over 2,000 years. Cement, aggregates, and water are the three primary components that go into concrete production, and approximately 70 % of the concrete's weight is made up of aggregates. Construction has increased the demand for natural aggregates. As natural resources deplete, it is necessary to offer some substitute materials for natural aggregates (Thomas, Damare and Gupta, 2013).

As automobile ownership increases, waste tires disposal is a critical environmental issue for communities throughout the world (Thomas, et al., 2014). Globally, 1.5 billion waste tires are discarded annually. This might reach 5 billion by 2030 (Chandra Gupta and Thomas, 2016). Since the number of cars in Malaysia is growing, waste tires have increased. This has resulted in environmental consequences in the future (Ling, Nor and Hainin, 2009). On the other hand, due to the constant increase in the number of waste tires manufactured over the years, the national department of solid waste management has given more attention to waste tire management (Chemisian Konsultant Sdn.Bhd, 2015).

There are numerous ways to dispose of tires, including landfill and burning. Tires containing styrene increase the risk of burns by releasing poisonous fumes that are hazardous to humans and the environment (Muñoz-Sánchez, Arévalo-Caballero and Pacheco-Menor, 2016). The problem with landfills is that they will destroy large areas of soil, contaminate the soil and groundwater due to the metal leaching from tires, and serve as mosquito breeding grounds (Kardos and Durham, 2015). Besides, waste tires cause a lot of "black pollution" because they do not break down easily and could harm the environment. One possible solution to this problem is reducing waste tires to a more valuable product, crumb rubbers. Rubberized concrete (RUC) is made by substituting fine aggregate partially with crumb rubber.

Concrete structures constructed in the 1960s and 1970s experienced durability issues like concrete cracking, freeze-thaw erosion, and chloride ions

penetration after 2 to 3 years of usage. Thus, in 1992, rubberized concrete was manufactured in the United States. At Arizona State University, Han Zhu's team constructed the world's first pavement test section using rubberized concrete, which exhibited outstanding performance in later use. Han Zhu has collaborated with the State of Arizona since 2000 to build several structural test sites using RUC (Xu, et al., 2020). These test locations have offered an essential experience for the continued application of rubberized concrete in engineering and continue to demonstrate excellent performance. According to studies, adding rubber to concrete improves its ductility and dynamic qualities. However, rubberized concrete's strength is lower than regular concrete, which restricts its use in construction.

2.1.1 Advantages of Rubberized Concrete

Rubberized concrete has several desired qualities, including low density, improved sound insulation, increased impact strength, and toughness (Ling, 2011). Rubber has a lower specific gravity compared to aggregates, so replacing aggregates with rubber will reduce the total specific gravity of rubberized concrete. In addition, rubberized concrete can effectively increase ductility and protect against damage caused by brittle fractures. Rubberized concrete possesses many beneficial properties, including resistance to acid, resistance to freeze-thaw cycles, resistance to chloride penetration, and enhanced damping ability (Kara De Maeijer, et al., 2021). These beneficial characteristics encourage the establishment of sustainable rubberized concrete to improve the environment. In addition to their positive effects on the environment, the advantages mentioned above make rubberized concrete ideal for civil engineering projects. For examples: lightweight concrete, non-load-bearing concrete walls, acoustic screens, improved insulation for building floors, reinforced concrete flat knit parapets, sidewalks, railroad beds, reinforced columns for seismic structures, high-impact rubber concrete beams, expansion joints in concrete slabs, and steel pipes filled with rubber concrete.

2.1.2 Application of Rubberized Concrete

The rubberized concrete application is mainly used in secondary or non-critical constructions. It can be utilised when strength is not as crucial because

it has a lower strength capacity than regular concrete. Rubberized concrete is applicable in architectural construction. Examples of architectural construction are nail concrete, sidewalks, green building precast roofs, jersey guards, and anti-slip ramps (Tomosawa, Noguchi and Tamura, 2005). Besides, rubberized concrete can be used for architectural light fixtures, decorative architectural elements, and building facades.

In addition, rubberized concrete can be used in regions with substantial freeze-thaw cycles. For instance, it can be utilised in locations with significant and frequent temperature changes, sports fields such as gymnasiums, tennis courts and basketball courts, airport waiting areas, leisure areas, and so on (Topçu and Demir, 2007).

Next, rubberized concrete resists noise and impacts well. It can be used in highway construction to offer impact absorption and blast barriers, as well as structural elements to preserve ductile reinforcement, which is vital in earthquake zones. Rubberized concrete can also be used in buildings to absorb shock waves from earthquakes (Topçu and Unverdi, 2018). In addition, it can be utilised in hydraulic structures such as dam spillways and tunnels when high abrasion resistance is required (Thomas and Chandra Gupta, 2016).

Last but not least, rubberized concrete can be used for mechanical foundation pads and railroad stations that need vibration dampening. It can also be used when an impact or blast resistance is needed. For example, trench filling, paving slabs, railroad buffers and shelters (Gerges, Issa and Fawaz, 2018).

2.2 Crumb Rubber

Crumb rubber (CR) refers to a material derived from waste tires that has undergone a process of size reduction and crushing, resulting in particles that range in size from 4.75 mm to 75 μm . In a specialised mill, waste tires are ground into 0.425 to 4.75 mm particles. The size of these particles is determined by the performance and temperature of the milling machine that ultimately produces them (Siddique, 2007). It replaces fine particles in concrete.

2.2.1 Processing of Crumb Rubber

There are numerous methods for recycling scrap tires, but the ideal method for tire rubber recycling is grinding it before converting it for other purposes. The waste tire can be separated into two categories which are automobile and commercial tires (Ganjian, Khorami and Maghsoudi, 2009). Researchers are typically more interested in automobile tires because they are produced in greater quantities than commercial tires. Table 2.1 shows the components of automobile tires, including the amounts of natural and synthetic rubber.

Table 2.1: Typical Contents of Automobile Tires (Li, et al., 2014).

Material	Content (%)
Natural rubber	14
Synthetic rubber	27
Black carbon	28
Fabric, Filler Accelerators & Antiozonants	16 - 17
Steel	14 - 15

Several activities are required to transform whole waste tires into smaller crumb rubber. Rubber can be ground into smaller pieces using four different techniques, which are normal temperature, freezing condition, wet condition and high temperature (Sienkiewicz, et al., 2012). The first method is grinding the rubber at room temperature using mills. The second method is grinding at ambient temperature under wet conditions. It involves using water to bring down the temperature, and the rubber particles are dried after the process is completed. The third method is grinding the rubber at a high temperature of roughly 130 degrees Celsius, where the rubber particles range in size from 1 to 6 millimeters and will be produced at the end of the process. The fourth method is known as grinding at freezing temperature, and it involves first chilling the rubber to a temperature lower than its original temperature, followed by placing it in a glass box and shredding it with an impact mill (Fawzy, Mustafa and Elshazly, 2020).

2.2.2 Properties of Crumb Rubber

Rubberized concrete is created by using rubber crumbs that range in size from 0.425 to 4.75 mm in concrete as a fine-aggregate substitute. Since crumb rubbers are lighter than fine aggregates, the replacement of crumb rubbers is usually performed based on their volume. Crumb rubber has a lower water absorption rate, strength, and stiffness than fine aggregates. The range of specific gravity values for crumb rubber falls between 0.51 to 1.2, and its bulk density is between 524 kg/m³ and 1273 kg/m³.

Crumb rubber is a substance that repels water and is non-polar in nature. That is resistant to water penetration and attracts air to its surface (Moustafa and ElGawady, 2015). In addition, its gradation is distinct from fine aggregates, which are below the particle size analysis curve. As a result, the gradation of the aggregate becomes discontinuous when it is utilised to substitute some of the fine aggregates in RUC.

Besides, crumb rubber can also be used to partially substitute coarse aggregates and cement according to their size. At first, the tires are processed through two phases as a replacement for coarse aggregate. In the first stage, the rubber is sliced into pieces measuring between 100 and 230 mm in length. Then, in the second stage, rubber granules measuring between 13 and 76 mm in size are produced that can be used as a partial replacement for coarse aggregate. Next, a micro-milling operation is necessary to lower the grain size from 0.075 mm to 0.475 mm as a partial substitution for cement.

2.3 Properties of Rubberized Concrete

Workability and bulk density of fresh rubberized concrete are important to determine its hardened qualities. Hardened properties of rubberized concrete include compressive, flexural and splitting tensile strengths, as well as impact resistance. Compressive strength is a material's capacity to sustain the axial force. When the ultimate compressive strength is reached, the material is crushed. Flexural strength is the maximum stress applied before the material fails. Splitting tensile strength is a material's capacity to resist tearing. Finally, impact resistance is the amount of energy concrete can withstand under intense force.

2.3.1 Workability

According to ASTM C125 (2007), workability is the effort necessary to manipulate freshly mixed concrete without losing homogeneity. In other words, the workability of concrete is the ease of mixing, handling and compaction. Several researchers discovered that the introduction of rubber had no significant impact on the workability of concrete (Gupta, Chaudhary and Sharma, 2016). Up to 10 % replacement of crumb rubber has minimal influence on workability, but an increase of replacement exceeding 10 % can significantly reduce the workability of the concrete (Moustafa and ElGawady, 2015). Besides, Oikonomou and Mavridou (2009) also reported that as the rubber's replacement grows up to 15 %, the slump value decreases and workability decreases. The decrease in workability is mainly due to the strong hydrophobicity of the crumb rubber. The strong hydrophobicity of the crumb rubber will further lead to segregation, reduced roughness and high specific surface of the rubber particles and increases the friction between the particles within the concrete. However, one study reported that the workability has increased to 50 % with the partial replacement of rubber crumbs with fine aggregates (Abdullah, Wan Zainal Abidin and Shahidan, 2016). The hydrophobicity of the crumb rubber, which repels water and increases the water available for the cement matrix, makes the rubberized concrete more workable and flowable.

2.3.2 Bulk Density

All research shows a reduction in bulk density for rubberized concrete. The density of rubberized concrete was 2 to 11 % less than regular concrete (Gesoglu, et al., 2014). Compared to a typical concrete mix, the density of rubberized concrete is often lower by roughly 20 % to 30 %, or approximately 1800 to 2100 kg/m³, depending on the specific circumstances (Siddika, et al., 2019). The bulk density declination is mainly because of the lower specific gravity of crumb rubber in comparison to natural aggregate. Besides, the hydrophobic behaviour of the rubber causes the crumb rubber concrete to become more porous. The air being trapped in the rubber's rough texture surface and the poor bonding of rubber particles to their surroundings will cause the bulk density of the rubberized concrete to decrease.

2.3.3 Compressive Strength

In general, RUC has a lower compressive strength than ordinary concrete. A reduction in strength of roughly 14 % to 89 % is observed in rubberized concrete (Marie, 2016). The same goes for other researchers. According to the findings, as the dosage of crumb rubber rose, the compressive strength decreased (Dong, Huang and Shu, 2013). Another study also reported that a reduction in compressive strength for 30 % rubber replacement to 35 MPa (Abdelmonem, et al., 2019). Due to the physical features of the rubber particles and their compatibility with tiny aggregates, rubberized concrete loses its strength. Besides, crumb rubber has a hydrophobic tendency. Therefore, adding more air to fresh rubber concrete mixtures causes the hardened rubberized concrete's void content to rise. This concentration of stresses throughout the structure causes microcracks to occur, lowering the concrete's strength.

2.3.4 Flexural Strength

Several researchers utilised crumb rubbers as a 20 % substitution for fine aggregates, resulting in a 12.8 % reduction in flexural strength. Additionally, the researchers observed in this investigation that as rubber particle size was reduced, the loss of flexural stiffness also decreased (Su, et al., 2015). Likewise, other researchers also discovered that adding crumb rubber to replace 5 % to 40 % of the fine aggregate decreased the flexural tensile strength by 4 % to 42 %. In fact, the flexural strength will be significantly reduced than its compressive strength because of the inadequate adhesion between cement paste and rubber particles (Ismail and Hassan, 2016).

2.3.5 Splitting Tensile Strength

Regardless of the size of the crumb rubbers, adding more rubber to the concrete mix diminishes splitting tensile strength. A study found that substituting fine and coarse aggregates for 10% to 40 % of crumb rubber reduced splitting tensile strength by 3 % to 49 % and 46 % to 73 % (Aslani and Khan, 2019). This decrease in splitting tensile is relevant for the same reasons that affect compressive strength. The crumb rubber particles function as a barrier and weaken the binding between the cement and rubber. Besides,

other studies had shown that the tensile strength dropped by 39.25 %, 48.30 %, and 52.45 % when 10 %, 20 %, and 30 % of the rubber was replaced with sand (Abdelmonem, et al., 2019).

2.3.6 Impact Resistance

Impact resistance depends on the toughness of the material and its ability to absorb impact loads. A study is available on the incorporation of rubber particles as a substitute for 10 to 30 % of the fine aggregates in concrete. As a result, with a crumb rubber quantity increase of up to 30 %, the impact resistance has increased by up to 12 % (Abdelmonem, et al., 2019). In addition, another study discovered that by adding 30 % crumb rubber to concrete, the impact energy raised it by 63 % (Balaha, Badawy and Hashish, 2007). Due to the addition of rubber to the concrete, the number of blows generated rose dramatically. Some other researchers pointed out that when compared to regular concrete, rubberized concrete provides a 50 % higher impact resistance (Hameed and Shashikala, 2016). In essence, the enhanced impact resistance results from the crumb rubber's energy absorption capacity.

2.4 Interface Transition Zone

As previously indicated, adding crumb rubber to concrete mixtures increases impact resistance. Nevertheless, it has a negative impact on the elastic modulus, compressive, splitting tensile and flexural strengths of concrete. The reduction is primarily because of the poor cement-rubber interface. The porous interfacial transition zone (ITZ) weakens cement matrix and aggregate bonding, which reduces the strength of RUC (Mohammed, et al., 2016).

Generally, scanning electron microscopy (SEM) is utilised to study the microstructure of crumb rubber and cement matrix by observing the variations of interfacial cracks. SEM images show poor adhesion and a small number of hydration products exist around the rubber particles at the ITZ (Gupta, Chaundhary and Sharma, 2014). Figure 2.1 shows a large gap between crumb rubber and the cement matrix, indicating a poor bond between rubber and cement particles. As a direct consequence, the interface cracks and reduces the overall strength of RUC. Several other researchers also pointed out that rubber particles do not adhere to the cement matrix as effectively in

comparison to the normal aggregate and significant fractures and gaps will occur surrounding the rubber particles (Dehdezi, Erdem and Blankson, 2015).

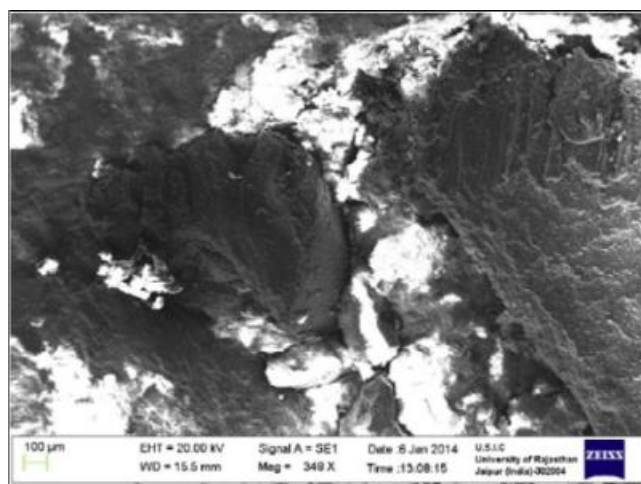


Figure 2.1: SEM Micrograph of ITZ With Magnification of 348× (Gupta, Chaundhary and Sharma, 2014).

In view of this, improving ITZ's strength is essential to reducing the strength loss driven by the porous weak cement matrix. Styrene-butadiene (SBR) latexes, often used as an adhesive, offer the potential to minimise strength loss by providing a bridging action in the intermediate transition zone.

2.5 Styrene-Butadiene Latex

The emulsion polymerization of monomers results in the formation of the latex polymer system, which is comprised of 50 % solids by weight. The most prevalent polymers found in latexes include styrene-butadiene, polyvinyl acetate, acrylic acid, and natural rubber. Concrete's mechanical properties, hydration process, and durability depend on its microstructure. Therefore, prior research has demonstrated that polymers as modifiers promise to improve the microstructure of concrete.

Styrene-butadiene rubber (SBR) latex is a polymeric dispersion emulsion comprised of butadiene, styrene, and water that bonds effectively to various materials. SBR has the appearance of a white, viscous liquid and has a good viscosity despite having a high water content of 52.7 %. It is utilised as a binder to enhance concrete's tensile, flexural, and compressive strengths. After hydration, the resultant hardened material has a continuous matrix of

interconnected solidified polymer particles that fill the gaps in the cement matrix and improves the bond between the cement paste and the aggregate.

In the United States, highway bridges have been constructed using mortar treated with SBR emulsion for the past 35 years. It is generally understood that latex-modified concrete is more durable than regular concrete. Due to its good chemical and mechanical resistance, it has been effectively employed during the past two decades as a repair material for concrete buildings, concrete bridges, road coverings, and waterproofing materials (Ohama, 1995).

2.5.1 Properties of Latex Modified Concrete

In order to increase the concrete's workability and durability, latex is added to concrete mixtures. The viscosity of latex aids in preventing cement and aggregate separation. Consequently, it improves the concrete's flexural and tensile strengths. The interaction between the surfactant and latex components is what causes the improvement of mechanical properties. Besides, the concrete's bonding strength is enhanced by the latex coating's development. Furthermore, most researchers recommend considering the optimum latex proportion in strengthening latex based concrete.

A study pointed out that with the addition of 5 % SBR by weight of cement, flexural strength was found to increase significantly (Li, et al., 2010). Essa, Amir and Hassan (2012) have examined the impact of adding SBR to cement paste and concrete. The inclusion of SBR affects early concrete strength negatively but later strength positively. The compressive strength increases as SBR content increases. In addition, according to that study, the flexural strength was improved by 7 %, 33 %, and 53 % at 28 days with the addition of 10 %, 25 %, and 35 % SBR to the concrete mix, respectively.

Similarly, Soni and Joshi (2014) also observed that the inclusion of latex affected the concrete's compressive strength negatively at an early stage. In contrast, the inclusion of SBR latex increased concrete strength after 28 days. The same pattern is seen in the flexural strength, which is decreased at early stages and is raised at 28 days of age with the addition of SBR latex. They also reported that the SBR latex provides a greater percentage increase in flexural strength when compared to compressive strength. Besides, they also

pointed out that the inclusion of SBR Latex raised the slump value of the concrete. The aforementioned observation indicates that SBR latex exerts a plasticizing influence on the concrete, thereby enhancing its workability.

The latex film formation, which maintains the internal pressure to continue the cement hydration process, is responsible for both the loss and gain in strength. In addition, it needs time to develop the latex film and the cement matrix. Therefore, the inclusion of SBR latex improves the compressive and flexural strength at 28 days of age due to the development of latex film with time. However, because the creation of latex film and cement hydration is still occurring in the early stage, the addition of SBR latex negatively impacts the concrete's strength.

In terms of splitting tensile strength, Doğan and Bideci (2016) found that SBR latex raised the splitting tensile strength by 13 %, 16 %, 17 %, and 25 %, at inclusion percentages of 1 %, 3 %, 5 %, and 8 %, in comparison to the control samples sample containing 0 % SBR. Thus, the tensile strength increases when the dosage of SBR latex used increases. Besides, the unit weight of concrete in samples with 1 %, 3 %, 5 %, and 8 % SBR latex dropped by 0.65 %, 1.31 %, 2.19 %, and 3.36 %, respectively, as compared to the control sample containing 0 % SBR. Thus, the fresh concrete unit weight of the control sample containing 0 % SBR is greater than that of the sample containing SBR.

Several studies have focused on the impact resistance of latex when combined with concrete. Notably, adding latex enhanced ordinary concrete's impact resistance by an average of 800 %. In addition, due to its ability to form the latex films inside the concrete matrix, latex gives the concrete some qualities that limit microcracks, perhaps enhancing its ability to withstand impacts (Soroushian and Tlili, 1991).

2.6 Latex Based Rubberized Concrete

Rubberized concrete is modified by SBR latex to enhance rubber-cement paste adhesion. It is believed that the rubber particles in latex based rubberized concrete (LRC) will improve rubber-cement paste adhesion. This may improve the mechanical characteristics of the microstructural alterations in latex based rubberized concrete.

SBR latex has excellent bonding capabilities and is compatible with rubber and cement matrix (R-CM) providing a chemical bond between crumb rubber and cement paste. Besides, SBR latex can make a three-dimensional latex film evenly distributed in the cement paste. This film can seal cement matrix voids, making the concrete more substantial, more flexible, more resistant to impact, and last longer (Xu, et al., 2014).

In most studies, the strength decreased when SBR latex was added to concrete. Nonetheless, the microstructural analysis yielded statistically significant improvements. Latex based rubberized concrete works better than regular rubberized concrete because it is more flexible. The rubber particles are spread uniformly throughout the cement paste to ensure consistent rubber distribution and a stronger connection between R-CM. The SBR latex will create a strong bond between the rubber and C-S-H, as a consequence, a gain in strength. Thus, a dense rubber-cement interface zone will be formed, and cement hydration products will be interspersed throughout the polymer film composites (Shen, et al., 2013).

2.6.1 Properties of Latex Based Rubberized Concrete

A study showed the density of LRC increased as the percentage of SBR latex utilisation was raised to 4 % (Ling, Nor and Hainin, 2009). This is primarily caused by the fact that adding SBR latex to the concrete mixture makes the concrete heavier because the amount of water increases.

Some other investigations have demonstrated that treating latex can improve the interfacial bond strength by increasing the surface activity of crumb rubber and the chemical bonds produced between the rubber and cement paste. Thus, the addition of latex to rubberized concrete leads to a notable enhancement in the material's toughness and a practical improvement in its strength (He, et al., 2021).

Following that, a study found that rubberized concrete treated with SBR latex resulted in a higher slump value than control mixes. This was because the fluidity and higher porosity of the SBR latex made the concrete mixes softer. Thus, compared to regular concrete, latex-modified rubberized concrete exhibit higher workability. Besides, SBR latex-modified rubberized concrete has a lower compressive strength than rubberized concrete without

SBR latex and the control mix. The strength reduced for 10 kg of latex-modified rubberized concrete was about 16.9 % compared with control samples (Grinys, et al., 2021). The loss of compressive strength is due to the excessive quantity of SBR latex, which increases the porosity of the concrete. This porosity causes the concrete to be less dense and the compressive force weaker.

Another study discusses the flexural and impact strength of latex based rubberized concrete. The researchers found that latex based rubberized concrete had higher flexural strength and impact resistance than regular and latex-modified concrete. The SEM images demonstrate that SBR latex produces a thin layer at the rubber-cement interface, strengthening the rubber-cement interfacial. Thus, the researcher concludes that due to the presence of SBR latex, the interfacial adhesion behaviour of R-CM is enhanced, which accounts for the increase in strength (Lee, et al., 1998).

Furthermore, Mohsin and Fahad (2015) pointed out that workability increases after adding SBR latex. This is primarily due to the increased consistency caused by the polymer particles' ball-bearing action between the cement particles. The improvement in flexural strength was also shown after the inclusion of SBR latex. The bond between the polymer film and cement hydrate is strengthened by SBR latex. This makes the latex-modified rubberized concrete more flexible and less likely to crack than regular concrete.

Other studies also reported that after modification by adding SBR latex into the LRC, concrete's compressive, splitting tensile, and flexural strengths had risen by 13.4 %, 21.8 %, and 25.5 %, respectively (Li, et al., 2014). In fact, latex can strengthen the binding between rubber and cement by acting as a surface modifier for rubber, improving the surface effect of rubber particles.

2.7 Steel Fiber

Most of the fibers used in cementitious composites are made of steel, glass, and polymers or sourced from natural substances. Steel, glass, synthetic, and natural fibers will impart unique qualities to concrete. Fibers can be more effective in preventing cracking than standard reinforcing steel because they

are spaced closer together. Typically, the weight of the fiber fraction is usually equal to 0.1 % to 3 % of the weight of the cement (Ansari and Sharma, 2017).

Fibers can be categorised into two groups according to their modulus of elasticity. Compared to cement mortar matrix, fibers such as steel, carbon, and glass have a greater modulus of elasticity, enhancing flexural and impact resistance. However, polypropylene and vegetable fibers are categorised as having a low modulus of elasticity, which can enhance the impact resistance of concrete but does not affect the flexural strength significantly (Behbahani, Nematollahi and Farasatpour, 2011) .

Because fibers come in different shapes and sizes, they can be used for many different things. For the flexural strength test, it is best to use longer fibers because longer fibers can be joined together to make stronger bonds that avoid additional bending. Most of the fibers are straight, but hooks on the ends of the metal ones are frequently seen since this enables fibers to lock into the concrete.

The most common type of fiber used to reinforce concrete is steel fiber (SF). At first, SF was used to restrict or regulate concrete's plasticity and shrinkage as it dried. More research and development have shown that adding SF to concrete can significantly improve its flexural toughness, energy absorption, ductility before final failure, cracking, and durability. Nowadays, construction is increasingly using steel fiber reinforced concrete. Some of these uses include the construction of road and airport pavements, hydraulic structures, fiber shotcrete, refractory concrete, and precast applications (Behbahani, Nematollahi and Farasatpour, 2011).

According to a study, the incorporation of steel fibers has been observed to significantly improve the compressive, flexural and splitting tensile strengths. In the study, the design mix without steel fiber inclusion exhibited the least compressive strength, while the design mix with 25 kg/m³ steel fiber inclusion demonstrated the highest compressive test result after 28 days. Regarding the flexural and splitting tensile strengths, the design mix with 40 kg/m³ steel fiber inclusion exhibits the greatest flexural and splitting tensile strengths when compared to the control mix and design mix with 25 kg/m³ steel fiber inclusion (Hafiz Ahmad and Awang, 2012).

Another study discusses the compression and flexural strength of steel fiber reinforced concrete. Tabassum, et al. (2018) pointed out that the compressive strength of concrete exhibits an increase of 18.4 %, while flexural strength exhibit an increase of 65.4 % with the inclusion of steel fiber content of 1.5 % and 2.0 %, respectively. However, subsequent increases in fiber content lead to a decrease in strength. The research findings indicate that a steel fiber content of 1.5 % is optimal for enhancing compressive strength, while content of 2 % is optimal for improving flexural strength.

Furthermore, Atoyebi, et al. (2018) pointed out that the splitting tensile strength of lighted weighted foam concrete decreased when the steel fiber inclusion was up to 0.4 %. However, the splitting tensile strength increased accordingly when the steel fiber inclusion of 0.6 %. The results suggested that the splitting tensile strength increases only when there is sufficient reinforcement. An insufficient quantity of steel fibers hinders the binding of the concrete rather than assisting it.

2.7.1 Properties of Steel Fiber Reinforcement Rubberized Concrete

Several studies have shown that adding granulated rubber to concrete mixtures makes the concrete more durable, flexible, and resistant to impact. However, it decreases the concrete's compressive, elastic modulus, splitting tensile, and flexural strengths. The strength diminished in RUC can be recovered by incorporating steel fibers to create steel fiber reinforced rubberized concrete (SFRC). A study reported that the inclusion of steel fibers enhances the compressive and flexural strengths (Wu, et al., 2016). However, the inclusion of crumb rubber and steel fibers in concrete poses a significant issue due to their negative impact on the mixture's freshness.

Eisa, Elshazli and Nawar (2020) have shown that the inclusion of steel fibers boosts the cohesiveness of the concrete mixture while decreasing its workability. As a matter of fact, steel fibers enhance internal friction within the concrete components. Additionally, the steel fibers have clumped together, restricting the aggregates' ability to move freely and decreasing workability. In this investigation, it was found that SFRC had a higher unit weight than regular rubberized concrete. The unit weight of the concrete mixture increased by roughly 2 % to 3 % due to the presence of steel fibers with a volume

percentage of 1 %. In addition, the inclusion of steel fibers increases the ability to bridge microcracks and limit crack expansion at an early stage. Consequently, the maximum compressive strength increases. The inclusion of hook-end steel fiber was discovered to improve the compressive strength by 7 %. Besides, when the percentage of rubber particles was 20 %, the incorporation of steel fibers increased the tensile strength and flexural strength by 75 % and 14 %, respectively. Adding steel fibers to concrete helps bridge microcracks and boost tensile strength at an early stage due to its high tensile strength.

Besides, another study gave the same result. The compressive and ultimate flexural strengths increased as the amount of fiber increased. At 90 days, regular concrete's compressive and ultimate flexural strengths were 105 MPa and 19 MPa, respectively. With 3 % straight steel fibers, the regular concrete's compressive and ultimate flexural strengths were increased to 150 and 35 MPa, respectively (Wu, et al., 2016).

Furthermore, Alsaif and Alharbi (2022) pointed out that the effect of rubber particles and steel fibers on workability was more significant when they were used together than when they were used separately, owing to the friction between the concrete components increases. For example, using 40 % steel fibers in the rubberized concrete resulted in a slump 32 % lower than regular concrete.

Abaza and Hussein (2016) indicated that steel fibers play a more significant role than rubber, and the incorporation of rubber and steel fibers improved the elasticity of concrete. Other studies also reported the impact resistance of SFRC has improved. During the test, the layer of granular rubber concrete performed admirably in terms of absorbing impact energy and safeguarding the SFRC layer from being damaged (Sukontasukkul, et al., 2013).

Few studies are available discussing that the tensile strength of rubberized concrete with a rubber volume percentage of 5 % rises as the steel fibers increase. It is possible that the steel fibers' ability to "bridge" the cracks in the concrete helped strengthen the rubberized concrete when pulled apart. The usage of steel fiber raised the splitting tensile flexural strengths of the rubberized concrete by 34.23 % and 86.96 %, respectively (Liu, et al., 2020).

Other studies also reported that including steel fiber would improve the rubberized concrete's impact resistance. The result demonstrated that adding 35 % crumb rubber and 1 % steel fiber enhanced the impact resistance of the concrete by a factor of 7.54 compared to the control mixture. This improvement shows that it might be possible to take advantage of the positive interaction between steel fiber and crumb rubber to create types of concrete that could be used in high-impact structural applications. This research also showed that the splitting tensile flexural strengths went up by an average of 20.5 % and 19.5 % when 0.35 % of steel fibers were added to SFRC mixtures compared to rubberized concrete (Ismail and Hassan, 2016).

2.8 Ordinary Portland Cement

According to ASTM C150 (2007), cement can be categorised into five major types, which are Type I, Type II, Type III, Type IV and Type V. Ordinary Portland Cement (OPC) is widely used as it has no limitation on the proportion of major oxides. So, it is used for general building projects, like reinforced concrete buildings, bridges, and pavements, where special properties are not needed and soil conditions are normal. Table 2.2 shows the chemical composition of the OPC.

Table 2.2: Contents of OPC (Marchment, et al., 2019).

Chemical	Content (%)
Al₂O₃	4.47
SiO₂	20.34
CaO	62.91
Fe₂O₃	4.58
K₂O	0.29
MgO	1.24
Na₂O	0.31
SO₃	2.58
LOI^a	3.27

2.9 Aggregate

According to ASTM C33/C33M (2018), aggregate can be divided into coarse and fine. Fine aggregate must be natural sand, artificial sand, recycled aggregate, or a combination. The fine aggregate must pass through no more than 45 % of the sieves, and its fineness modulus must be between 2.3 and 3. Coarse aggregate must be composed of gravel, crushed gravel, crushed stone, air-cooled blast furnace slag, crushed hydraulic-cement concrete, other recycled material, or a mix thereof, meeting the requirements of this standard.

2.10 Superplasticizer

According to ASTM C494/C494M (2019), high-range water reducing (superplasticizer) is classified as Type F and G. Superplasticizers (SP) are admixtures introduced in extremely small amounts to the concrete mixture. The amount of superplasticizer incorporated into concrete significantly affects the performance of concrete. Superplasticizer is commonly utilised in concrete and has become a standard component of concrete. Superplasticizers enhance the fluidity of concrete by spreading the cement particles inside the mixture. Their incorporation significantly improves the mixture's workability. The compatibility of RUC reduces as the percentage of rubberized sand increases. Adding superplasticizers to rubberized concrete may thereby increase the workability of rubberized concrete.

Hamouda (2015) pointed out that with an increase in the amount of superplasticizer, the workability of concrete is greatly enhanced. Because the water-reducing chemical generates the same electrostatic charge on the cement particles' surface, it causes cement particles to repel one another, preventing agglomeration and minimising air entrainment. Thus, the concrete particles become easier to move around, and water that is not limited by the flocculation system can be used to lubricate the mixture, which makes the mixture easier to work with. As a result, the workability increases.

Furthermore, some other researchers also reported that superplasticizers could increase the air content while simultaneously adjusting the workability of the concrete (Ismail and Hassan, 2016). Similarly, Bisht and Ramana (2017) also reported that adding the superplasticizer can compensate for the decrease in workability produced by crumb rubber in the concrete.

2.11 Silica Fume

Most of the aforementioned studies showed that adding crumb rubber as aggregates made the mechanical properties of concrete even worse. But ultrafine mineral admixtures, like silica fume, are said to make the cement paste more uniform and reduce the number of the void, both of which make the concrete stronger. According to ASTM C1240 (2020), silica fume known as microsilica, is fine pozzolanic substance. There is also good evidence that adding silica fume makes the cement-aggregate interface denser. The silica fume increased adhesion and reduced weak regions at the cement-rubber interface, as shown in Figure 2.2. As a result, making use of silica fume as an alternate technique to enhance the behaviour of rubberized concrete in structural applications.

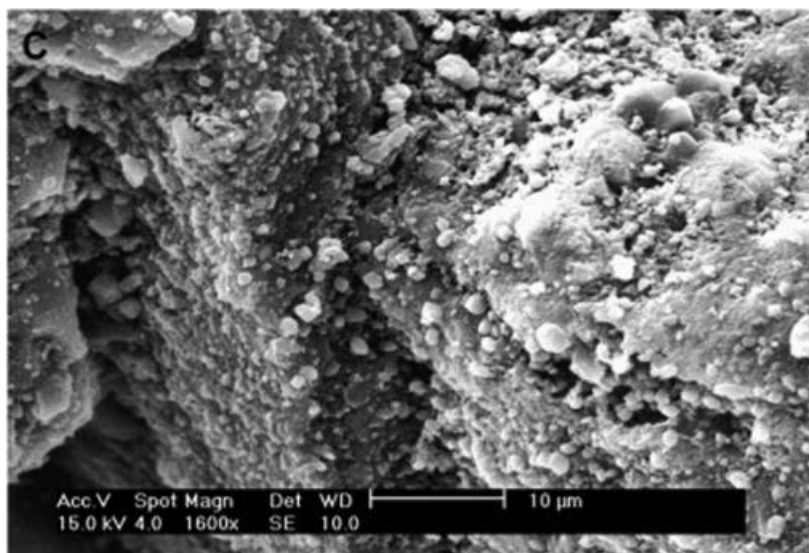


Figure 2.2: Silica Fume on the Rubber Particle (Xu, et al., 2020).

Several researchers were concentrating on adding silica fume into the rubberized concrete. Most of the test findings demonstrated that when the rubber content grew from 0 % to 50 %, the compressive and splitting tensile strengths and the elastic modulus gradually declined. But adding silica fume to plain concrete, especially rubberized concrete, will improve the mechanical properties and slows down the strength loss that comes with adding rubber. This silica fume has caused a significant positive impact on compressive and

splitting tensile strengths, resulting in up to 43 % and 27 % strength improvements, respectively (Güneyisi, Gesoğlu and Özturan, 2004).

Besides, Xue and Shinozuka (2013) reported that adding silica fume at all replacement rates consistently raised the compressive strength by 3 MPa to 7 MPa. The addition of silica fume to rubberized concrete was discovered to strengthen the binding between rubber and cement, enhancing the hydration and crystallisation surrounding the rubber particles. Silica fume can promote C-S-H nucleation to make the microstructure around the rubber particles more homogeneous. Thus, the good bonding between the rubber crumb and cement paste leads to higher compressive strength in rubberized silica fume concrete.

In terms of density, Pelisser, et al. (2011) said that rubberized concrete was 13 % less dense than regular concrete, but when silica fume was added to the rubberized concrete, it only lost 9 % of its density because the structure of the concrete was already very dense when the silica fume is added.

Some other researchers pointed out that replacing fine aggregates with rubber fibers and cement with silica fume can bring a positive effect on impact resistance. Gupta, Sharma and Chaudhary (2015) indicated that when silica fume is used to replace some of the cement in concrete, the number of cracks is minimised, and the performance of high strength concrete under impact and fatigue loading is improved. Besides, Silica fume also makes concrete with polypropylene fibers more resistant to impact by helping the dispersion of fibers.

2.12 Summary

Rubberized concrete (RUC) is a type of concrete mixture that incorporates crumb rubber particles as a substitute for fine or coarse aggregate. It offers better flexibility, toughness and impact resistance. However, literature reviews also show that the introduction of crumb rubber induces lower compressive, split tensile and flexural strengths. The reduction is primarily due to the poor interfacial performance of rubber-cement matrix.

Styrene-butadiene (SBR) latex, which is often used as an adhesive, offers the potential to minimise strength loss by providing a bridging action in the intermediate transition zone (ITZ). Rubberized concrete is modified by SBR latex to form Latex based rubberized concrete (LRC). Latex based

rubberized concrete works better than regular rubberized concrete because it is stronger, more flexible, more resistant to impact and lasts longer.

Besides, adding steel fiber to the concrete during the manufacturing process to form SFRC can also address the problem of low strength for the RUC, as the steel fibers can bridge microcracks and limit crack expansion. However, the incorporation of rubber granules and steel fibers will negatively affect the fresh properties of concrete. Thus, admixtures such as superplasticizers and silica fumes can be added to increase workability. However, despite increased workability, silica fumes can also improve adhesion between the crumb rubber and the cement, enhancing the performance of the concrete.

CHAPTER 3

METHODOLOGY AND WORK PLAN

3.1 Introduction

The study's methodology is covered in this chapter. The complete process, from the preparation of the raw material and mixing procedures to the testing method, is described in detail. All the processes are in accordance with BS EN and ASTM standards to make sure the consistency and accuracy of the data.

3.2 Flow Chart of the Study

Figure 3.1 shows the design flow chart for the study of latex based rubberized concrete with 15 kg/m³ steel fiber.

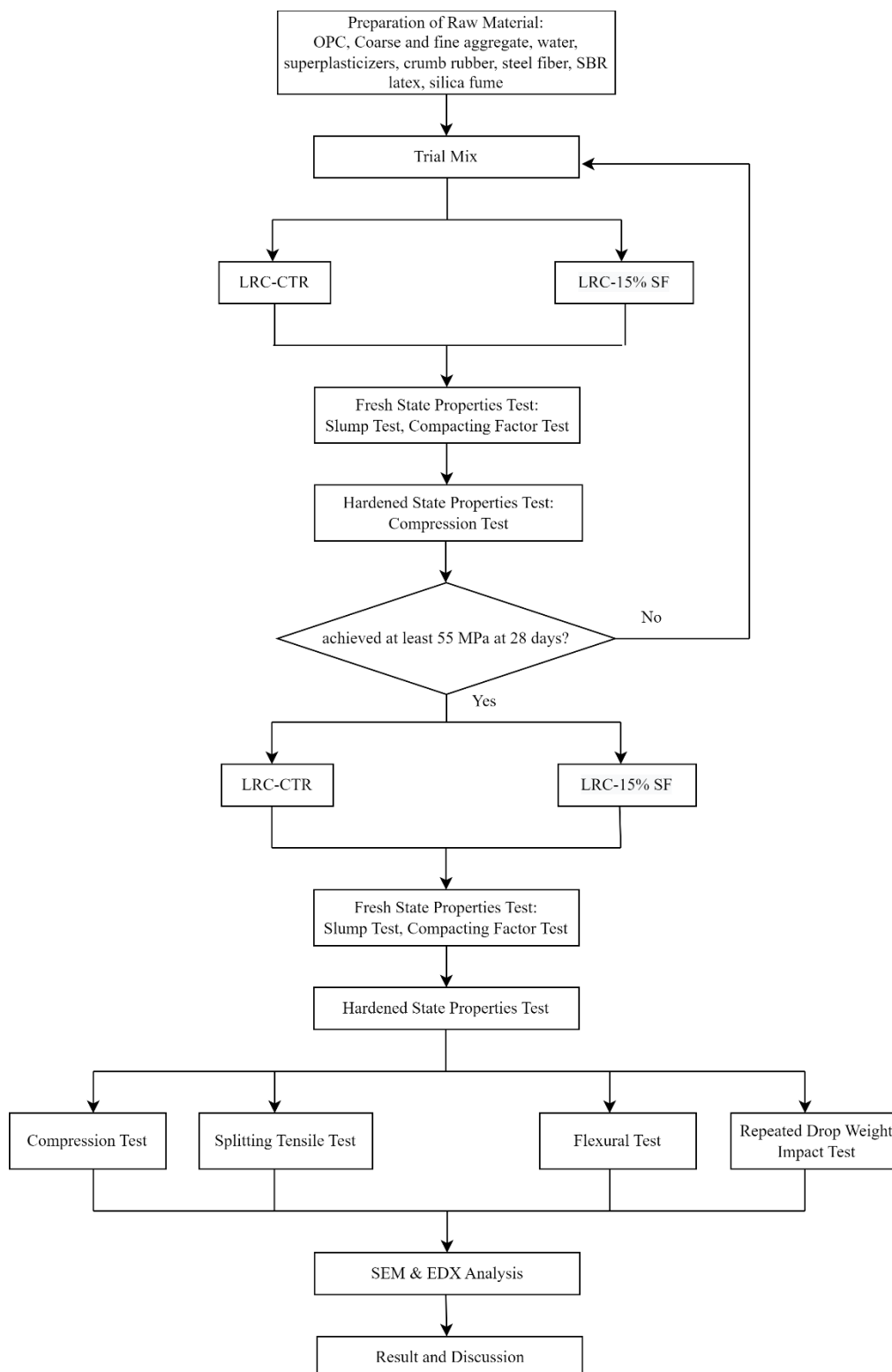


Figure 3.1: Design Flow Chart.

3.3 Raw Material

This study used materials including Ordinary Portland Cement (OPC), coarse and fine aggregates, water, superplasticizer, crumb rubber, Styrene-Butadiene (SBR) latex, silica fume and steel fiber.

3.3.1 Ordinary Portland Cement (OPC)

The cement used is Type 1 Ordinary Portland Cement (OPC). The cement utilised in this study was manufactured and supplied by YTL Cement Sdn Bhd under the commercial brand name Orang Kuat. Orang Kuat, CEM I branded cement meets the strength class of 52.5 N and is certified to MS EN 197-1:2014. Therefore, it can be used in places where high-strength concrete is needed and is in compliance with MS ISO 9001, MS ISO 14001, OHSAS 18001 and MS ISO 50001 (YTL Cement, 2022). Figure 3.2 illustrates the YTL Orang Kuat branded cement, while Table 3.1 shows the properties of YTL Orang Kuat, CEM I branded cement. Besides, the typical chemical composition and bogue compound composition of 52.5 N OPC (Type 1) are presented in Table 3.2 and Table 3.3, respectively.



Figure 3.2: YTL Orang Kuat, CEM I Branded OPC.

Table 3.1: Properties of YTL Orang Kuat, CEM I Branded OPC (YTL Cement, 2022).

Tests	Units	Specification MS EN		Test Results
		197-1: 2014 CEM I 42.5N		
Chemical Composition				
Insoluble Residue	%	≤ 5.0		0.4
Loss On Ignition (LOI)	%	≤ 5.0		3.2
Sulfate Content (SO₃)	%	≤ 3.5		2.7
Chloride (Cl⁻)	%	≤ 0.10		0.02
Physical Properties				
Setting Time (Initial)	Mins	≥ 60		130
Soundness	Mm	≤ 10		1.2
Compressive Strength	MPa	≥ 10		29.7
(Mortar Prism)	MPa	$\geq 42.5; \geq 62.5$		48.9
(1:3:0.5)		: 28days		

Table 3.2: Typical Chemical Composition of 52.5 N OPC (Type 1)
(Kanadasan, et al., 2015).

Oxides	Composition (%)
Al₂O₃	5.37
CaO	64.00
Fe₂O₃	2.94
K₂O	0.17
MgO	3.13
Mn₂O₃	0.24
Na₂O	0.12
SiO₂	20.29
SO₃	2.61
P₂O₅	0.07
TiO₂	0.12
Others	0.94
Loss on ignition	1.40

Table 3.3: Bogue Compound Composition of 52.5 N OPC (Type 1)
(Kanadasan, et al., 2015).

Bogue Compound	Composition (%)
C₃S	58.62
C₂S	13.95
C₃A	9.26
C₄AF	8.95

Prior to mixing, the OPC was sieved through a 0.3 mm sieve as shown in Figure 3.3, to eliminate any lumps. After that, the sieved OPC was stored in an air-tight container as shown in Figure 3.4, to avoid contact with moisture from the environment.



Figure 3.3: Sieving of OPC.



Figure 3.4: Sieved OPC in an Air-Tight Container.

3.3.2 Coarse Aggregate, Fine Aggregate and Crumb Rubber

The coarse and fine aggregates used in this study were provided by local suppliers. The fine aggregates were the river-washed fine aggregates, which had a fineness modulus of 2.18. Any coarser particles that remained on the 2.36 mm sieve after the fine aggregates had been sieved through it were

eliminated. Figure 3.5 shows the fine aggregates retained on the receiving pan. Next, the coarse aggregates utilised in this study were a 3/4 inches aggregate with a specific gravity of 7.06. The coarse aggregates were sieved through a 20 mm sieve, a 10 mm sieve, and a 1.18 mm sieve. The particles retained on the 20 mm sieve and passed through the 1.18 mm sieve were eliminated. After that, to eliminate the initial moisture in the pores and make sure that all mixes had a constant W/C ratio when water was added, both fine and coarse aggregates were oven-dried at a temperature of $(105 \pm 5) ^\circ\text{C}$ for 24 hours. Figure 3.6 illustrates the coarse and fine aggregates oven-dried in an oven.



Figure 3.5: Fine Aggregates Retained on the Receiving Pan.



Figure 3.6: Coarse and Fine Aggregate Oven-Dried in the Oven.

Crumb rubber was utilised to substitute the fine aggregate by weight. The crumb rubbers utilised in this study were natural rubber granules from Yongfeng Rubber, a local supplier that in accordance with ASTM D5644 (2018), ASTM D1509 (2018) and ASTM D5603 (2019) to make sure the quality of the rubber in terms of passing rate, heat loss, metal content, and fiber content. The crumb rubber ranged in size from 1 to 4 mm and has a fineness modulus of 4.62. Figure 3.7 illustrates the crumb rubbers used throughout this study.



Figure 3.7: Crumb Rubbers.

Besides, the sieve analysis was conducted according to ASTM C 33. The particle size distribution of coarse and fine aggregate, as well as crumb rubber were determined by sieve analysis. At first, 1000 g of coarse aggregate, 500 g of fine aggregate and 500 g of crumb rubber were weighted. The coarse and fine aggregate were then dried in an oven at 105 °C. For coarse aggregate, the sieves were stacked with the largest of 25 mm at the top and the smallest of 5 mm at the bottom. For fine aggregate and crumb rubber, the sieves were stacked with the largest of 4.76 mm at the top and the smallest of 150 μm at the bottom for fine aggregate and crumb rubber. The sample was placed on the top sieve while the sieve was placed on the sieve shaking machine. The apparatus of the sieve analysis test is shown in Figure 3.8. The cover plates were tightened and the timer was set to 15 minutes after the machine was switched on. The material retained in each sieve was weighted and the percentage by weight of the total sample passing through each sieve was calculated. The results of sieve analysis for coarse aggregate, fine aggregate and crumb rubber are presented in Appendix A-1, Appendix A-2 and Appendix A-3, respectively.

After that, the grading curve was plotted and the fineness modulus of a coarse and fine aggregate, as well as crumb rubber were calculated. Figure

3.9 shows the particle size distribution curve of coarse and fine aggregate, as well as crumb rubber. The fineness modulus of coarse and fine aggregate, as well as crumb rubber are tabulated in Table 3.4.



Figure 3.8: Set Up of Sieve Analysis Test.

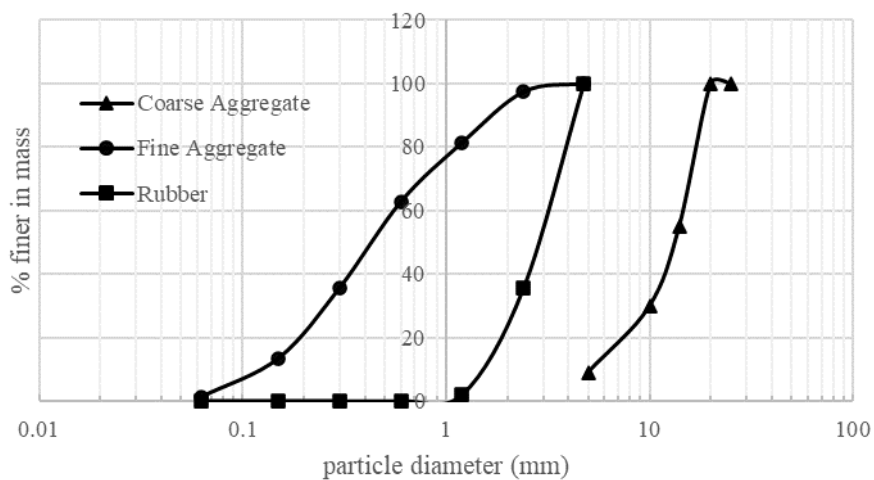


Figure 3.9: Finer in Mass Against Particle Size.

Table 3.4: Fineness Modulus of Coarse Aggregate, Fine Aggregate and Crumb Rubber.

Material	Fineness Modulus
Coarse Aggregate	7.06
Fine Aggregate	2.18
Crumb Rubber	4.62

3.3.3 Water and Superplasticizer

The water used for mixing and curing is the municipal water supply's pure tap water in complies with ASTM C1602/C1602M (2022). To make sure that the hydration process and subsequent strength of the concrete were not impacted, the water must be free from sediment, impurities and chemicals. This is because the impurities will affect the setting and hardening properties of the concrete. The specific gravity of the water used for mixing and curing was assumed to be 1.0 and must be kept at room temperature (27°C).

Next, the superplasticizer (SP) acted as a water reducing agent and was mixed into the concrete mixture. The SP was supplied by the local supplier, BASF as shown in Figure 3.10. Superplasticizer was utilised to maintain the great workability of the fresh mix without losing its strength. The amount of the superplasticizer used varied depends on the amount of water and latex used in the concrete mix.



Figure 3.10: BASF Superplasticizer.

3.3.4 Styrene-Butadiene (SBR) Latex

Latex was used in this study as an additive. SBR latex was utilised and developed specifically for cement production as a useful bonding agent. SBR latex is a milky white liquid latex mostly made up of styrene, butadiene, and water. Figure 3.11 illustrates the Styrene-Butadiene (SBR) Latex used throughout this study. Before mixing, the SBR latex was stirred well to prevent any settlement at the bottom. Then, crumb rubbers were added and coated well with the SBR latex on its surface.



Figure 3.11: Styrene-Butadiene (SBR) Latex.

3.3.5 Silica Fume

The primary objective of including silica fume into the mix was to make up for the probable reduction in the material's strength that results from the use of crumb rubbers to replace the fine aggregates. A kind of silica fume that was supplied by Scancem Materials Sdn. Bhd., was utilised in this study. It is mostly made up of amorphous silica, iron oxide, calcium magnesium carbonate and crystalline silica. Figure 3.12 illustrates the silica fume utilised throughout this study.



Figure 3.12: Silica Fume.

3.3.6 Steel Fiber

The steel fiber utilised in this study was STAHLCON hooked-end steel fiber HE 0.55/35 as shown in Figure 3.13. It is a bundle of steel fibers with hooks at the ends that help mix the concrete. It is mainly produced by cold-drawn wire in compliance with BS EN 14889-1 (2006). Both ends hooked glued steel fiber with a density of 15 kg/m^3 are utilised in this study. Table 3.5 summarises the properties of steel fiber HE 0.55/35.



Figure 3.13: Stahlcon Hooked-End Steel Fiber HE 0.55/35.

Table 3.5: Properties of Stahlcon Hooked-End Steel Fiber.

Properties	HE 0.55/35
Fiber Diameter	0.55 mm (\pm 0.03 mm)
Fiber Length	35 mm (\pm 1.75 mm)
Aspect Ratio	65 (\pm 4.5)
Tensile Strength	Min 1200 MPa (\pm 5 %)

Tensile test was conducted according to ASTM A370 (2022) to investigate the mechanical properties of steel fiber and their potential for reinforcing concrete. The Shimadzu Universal Testing machine was used to conduct the tensile test. Firstly, the Shimadzu Universal Testing machine was powered on and the grip head was installed to the load cell. The computer which connected to the Shimadzu testing machine was turned on and the test method was set to tensile type. After that, the force direction and dimension of steel fiber were set into the test file method. The loading rate of the tensile test was set to 1 mm per minute. Before the start of the test, the Shimadzu testing machine was calibrated by using computer to ensure the accuracy of the test. Then, the steel fiber was gripped to the grip head as shown in Figure 3.14. After that, the tensile test was started. The failure of steel fiber indicated the

end of the test. The steel fiber will failed and break into two parts. The testing results were save and exported in pdf and excel file format.



Figure 3.14: Preparation of Tensile Test.

3.4 Concrete Mould

Different concrete moulds were used to prepare different specimens for the different strength tests. Cubic mould was used for the compression test. Next, cylindrical mould was used for the splitting tensile test, while prism mould was used for the four point loading flexural test and repeated drop weight impact test. Figure 3.15, Figure 3.16 and Figure 3.17 illustrate the cubic mould, cylindrical mould and prism mould, respectively. The summary of the particular mould with its dimension and the required test is shown in Table 3.6. The dimension of the moulds were all in complies with BS EN 12390-1 (2021) and ASTM C31/C31M (2022).



Figure 3.15: Cubic Mould.



Figure 3.16: Cylindrical Mould.



Figure 3.17: Prism Mould.

Table 3.6: Summary of the Mould Used for Test.

Mould	Dimension (mm)	Strength Test
Cubic	150 × 150 × 150	Compressive Strength Test
Cylindrical	100 × 200	Splitting Tensile Strength Test
Prism	100 × 100 × 500	Flexural Strength Test, Repeat Drop Weight Test

Prior to actually pouring in the fresh concrete, the moulds should be cleaned with the scrapper and brusher to ensure no residue is left inside. Besides, the mould should be locked firmly using the spanner and cleaned again using the air blower as shown in Figure 3.18. Then, a layer of oil should be coated on the inner surface of the mould using a brusher to enable the ease of demoulding. Figure 3.19 illustrates applying of a thin oil layer on the mould's surface.

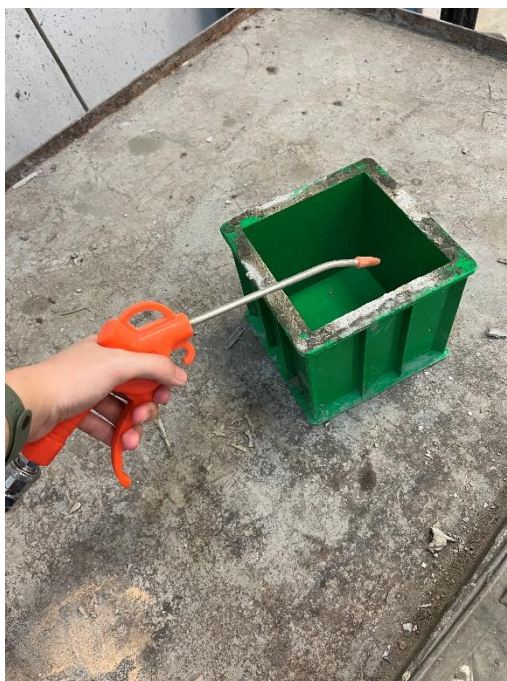


Figure 3.18: The Mould Was Cleaned With Air Blower.



Figure 3.19: A Thin Layer of Oil Was Coated on the Mould's Surface.

3.5 Trial Mix

Trial mix is important and must proceed prior to casting for the real mix specimen in the study. The trial mix of latex based rubberized concrete (LRC) and latex based rubberized concrete with 15 kg/m^3 steel fiber (LRC-15 % SF) were needed to proceed to reach the 28 days cubic compressive strength of 55

MPa. This is because the concrete to be used must have at least 55 MPa of cubic compressive strength at 28 days to make sure the stresses are transferred and serviced within the allowable values in compliance with BS EN 206-1 (2001). Thus, the trial mix of cubic specimens for LRC and LRC-15 % SF were prepared and cured for 7 days and 28 days. The W/C ratio for the trial mix of LRC was designed to have a range from 0.28 to 0.32 with a 0.02 interval of increment, while the W/C ratio for the trial mix of LRC-15 % SF was designed to also have a range from 0.28 to 0.32 with a 0.02 interval of increment. In short, thirty-six cubic specimens were needed to prepare for compression test. Lastly, the optimum combination of the trial mix for both LRC and LRC-15 % SF had achieved at least 55 MPa of 28 days characteristic strength was chosen to test for the compressive, splitting tensile and flexural strengths, as well as impact resistance in this study.

3.6 Mixing Procedure

The mixing procedure was carried out with the help of concrete mixer in this study. For LRC-15 % SF, at first, the amount of OPC, sand, coarse aggregate, crumb rubber, silica fume, superplasticizer, latex and steel fiber needed were weighted out by a weighing machine to give mixes of specific proportion by weight. For example, Figure 3.20 shows the fine aggregate was weighted using the weighing machine. Then, the crumb rubber was added to the SBR latex to coat its surface with the latex as shown in Figure 3.21. After that, all the OPC, fine aggregate, coarse aggregate, crumb rubber coated with SBR latex and silica fume were added into a concrete mixer accordingly and mixed well to form the dry mix. Later, the SBR Latex was added to the water. The water together with the SBR latex were then poured into the dry mix part by part. The mixing was carried out until the mix was uniformly mixed and formed mortar. Lastly, the steel fiber was added to the fresh concrete mortar in few times. However, for LRC, the mixing procedure was similar to that of LRC-15 % SF except the last step, which was adding steel fiber, was not required.



Figure 3.20: Fine Aggregate Was Weighted.



Figure 3.21: Crumb Rubber Coated With SBR Latex.

3.7 Fresh State Properties Test

Fresh properties test was conducted prior to actually placing the fresh concrete into the concrete mould to ensure the workability and quality of the concrete.

A slump test and compacting factor test were performed in this study to study the fresh properties of the concrete.

3.7.1 Slump Test

Slump testing was performed in accordance with ASTM C143/C143M (2020). A 5/8 inches diameter and 24 inches long steel tamping rod, slump cone, large pan, ruler and trowel were prepared. The slump cone (frustum mould) with a height of 300 mm was placed on a smooth, flat, moist and non-absorbent surface. The 200 mm diameter base was set on a flat surface, with a smaller 100 mm diameter opening on top. Next, fresh concrete was poured into the frustum mould in three layers, with about one third of the mould's volume in each layer. The tamping rod consolidated the fresh concrete mix by tapping with 25 times even strokes in each layer of fresh concrete as shown in Figure 3.22. After that, the excessive fresh concrete on the top surface was struck off. Then, the frustum mould was slowly lifted in a vertical direction by roughly 300 mm. All these steps were recommended to be finished in 2.5 minutes. Lastly, the slump cone was placed beside the slumped concrete, and a tamping rod was placed on the top of the cone. The difference between the height of the frustum mould and the height of the slumped concrete was used to figure out the slump value. The slump value must be determined immediately after the mould was removed. Figure 3.23 illustrates the slumped concrete (LRC) produced by the slump test.



Figure 3.22: Concrete Mix Was Consolidated Using Tamping Rod.



Figure 3.23: Slumped Concrete.

3.7.2 Compacting Factor Test

The compacting factor test was another method used to examine the workability of fresh concrete. Compacting factor test was carried out in compliance with BS EN 12350-4 (2019). The purpose of this test was to measure the ability of fresh concrete to flow and fill all the spaces within the

formwork without segregation or bleeding. The compacting factor test measured the ratio of the weight of fully compacted concrete to the weight of partially compacted concrete. At first, the fresh concrete was transferred to the upper hopper until full. Then, the trapdoor of the upper hopper was opened to allow the concrete to fall to the lower hopper. After that, the trapdoor of the lower hopper was opened to allow the concrete to fall into standard cylindrical mould. Then, the fresh concrete in the cylinder was compacted by using a tamping rod until fully compacted. The cylinder with fully compacted concrete was weighted. Repeated the steps above without compacting the concrete in the cylinder. Then, the cylinder with partially compacted concrete was weighted. Lastly, the compaction factor was calculated by using Equation 3.1. Figure 3.24 shows the apparatus of the compacting factor test.

$$\text{Compacting Factor} = \frac{\text{Partially compacted concrete}}{\text{Fully compacted concrete}} \quad (3.1)$$



Figure 3.24: Compacting Factor Test.

3.8 Casting Procedure

After that, the fresh concrete was transferred to different concrete moulds such as cubic mould, cylinder mould and prism mould. The prismatic mould (100 mm × 100 mm × 500 mm) was used for repeated drop weight impact test and flexural test. The cylindrical mould has a diameter of 100 mm and a height of 200

mm was used for the splitting tensile test. The cubic mould has dimensions of 150 mm × 150 mm × 150 mm was used for the compression test. Prior to casting, all the moulds should be cleaned, screwed and applied with a thin layer of oil. The fresh concrete was added into the mould by 3 layers, then each layer needed to be consolidated by 25 strokes using the standard 5/8 inches diameter tamping rod in order to release trapped air in the fresh concrete. Subsequently, the recently mixed concrete was left in the mould overnight to let it set. Figure 3.25 illustrates that the fresh concrete was transferred to the prism mould.



Figure 3.25: Fresh Concrete Was Transferred to the Prism Mould.

3.9 Curing

After one day, the concrete specimens were demoulded and labelled. Then, water curing was conducted for all the concrete specimens. According to ASTM C31/C31M (2022), the surface of the concrete specimens should be preserved with water at all times during the curing process. During the curing process, the cubics, cylinders, and prisms specimens were placed in a water tank with a thick cover as shown in Figure 3.26. The temperature of the curing water must be maintained between 24 °C to 28 °C throughout the process. After exactly 7 days, 28 days and 56 days, the concretes were oven-dried for 1 hour after being removed from the water tank. Then, the dimension of the concrete specimens were measured three times to get the average value, and the weight

of the concrete specimens were measured using a weighing machine as illustrated in Figure 3.27 and Figure 3.28, respectively.



Figure 3.26: Water Curing for the Concrete Specimens.



Figure 3.27: Dimension Was Measured Using Vernier Calliper.



Figure 3.28: Concrete Was Weighted Using Weighing Machine.

3.10 Hardened State Properties Test

There are two types of hardened concrete testing which are destructive tests and non-destructive tests. In this study, destructive tests including compression test, splitting tensile test, flexural test and impact test were performed to determine the mechanical properties of the LRC and LRC-15 % SF. After the curing process, the concrete sample was oven-dried for 1 hour. Then, the weight of concrete specimens were taken and the dimension were measured to calculate the bulk hardened density by using Equation 3.2.

$$\rho = \frac{W}{V} \quad (3.2)$$

where

ρ = bulk hardened density, kg/m³

w = mass of the specimen, kg

v = volume of the specimen, m³

3.10.1 Compression Test (BS EN 12390-3)

The compression test was performed as per BS EN 12390-3 (2019). The cubic specimens were required for the compression test. Before testing, the concrete was oven-dried for 1 hour after being removed from the water tank. Then, the specimens' weight and dimension were measured using a Vernier calliper and digital weighing scale, respectively. The test was conducted utilising the universal compression test machine under a loading rate of 6 kN/s. The centre of the concrete specimen was placed aligned with the base plate of the machine. The specimen was then loaded at a constant rate until it broke. When that happens, the maximum load was written down to calculate the compressive strength based on Equation 3.3. Figure 3.29 illustrates the equipment and setup of the compressive strength test.

$$f_c = F/A_c \quad (3.3)$$

where

f_c = compressive strength, MPa

F = maximum load subjected to the specimen, N

A_c = cross sectional area of the specimen subjected to applied load, m²



Figure 3.29: Compressive Strength Test.

3.10.2 Splitting Tensile Test (BS EN 12390-6)

The splitting tensile test was performed in compliance with BS EN 12390-6 (2010). The cylindrical specimens were used for the splitting tensile test. Before testing, the concrete was oven-dried for 1 hour after being removed from the water tank. Then, the specimens' weight and dimension were measured using a Vernier calliper and digital weighing scale, respectively. The test was performed utilising the compression test machine at a loading rate of 1.5 kN/s. A diameter line should be drawn carefully on each specimen. Then, the packing strips were positioned along the top and bottom of the specimen's loading face with centers on the lines marked on the ends of the cylinder. Packing strips were used to ensure the applied load could be distributed uniformly along the cylindrical specimen. Throughout the loading process, it must be made sure that the specimen remains in the centre. The constant loading rate was applied on the horizontal side of the concrete specimen until a 'pop' sound was heard, which indicates failure and shattering of the specimen. Finally, the maximum load that the specimen was able to withstand was recorded. The calculation of the splitting tensile strength was performed based on Equation 3.4. Figure 3.30 illustrates the equipment and setup of the splitting tensile test.

$$T = \frac{2P}{\pi LD} \quad (3.4)$$

where

T = splitting tensile strength, MPa

P = maximum applied load, N

L = length of the cylindrical specimen, mm

D = diameter, mm



Figure 3.30: Splitting Tensile Strength Test.

3.10.3 Flexural Test (BS EN 12390-5)

The flexural test was conducted in compliance with BS EN 12390-5 (2019). The prism specimens were used for the flexural test. Before testing, the concrete was oven-dried for 24 hours after being removed from the water tank. Then, the specimens' weight and dimension were measured using a Vernier calliper and digital weighing scale, respectively. The test was conducted utilising the Concrete Flexural Test Machine with a loading rate of 0.15 kN/s. Four vertical lines were drawn with 120 mm spacing and 70 mm spacing from both ends on the prism specimen. A constant loading rate was applied until the prism specimen was cracked. The test result was recorded, and the flexural strength was calculated using the third point loading method based on Equation 3.5. Figure 3.31 illustrates the equipment and setup of the flexural strength test.

$$R = \frac{PI}{BD^2} \quad (3.5)$$

where

R = flexural strength, MPa

P = maximum load applied, N

I = distance between the supporting rollers, mm

B = width of specimen, mm

D = depth of specimen, mm



Figure 3.31: Flexural Strength Test.

3.10.4 Repeated Drop Weight Impact Test

The repeated drop weight impact test was conducted in compliance with ACI 544 (1996). In this study, the prism specimens were used for the two types of repeated drop weight impact tests. At first, the test was carried out to drop a 2 kg mass from the height of 200 mm on the prism concrete specimen with a span length of 400 mm. Then the half split prism specimen concrete for the first impact test was continued for the second impact test. The second test was carried out to drop a 2 kg mass from the height of 300 mm on the half split prism concrete specimen with a span length of 200 mm. After that, the number

of drops required to create the final fracture was recorded. The impact resistance of the concrete was determined by calculating the impact energy, which is the potential energy absorbed based on Equation 3.5. Figure 3.32 illustrates the equipment and setup of the repeated drop weight impact test.

$$E_{impact} = Nmgh \quad (3.5)$$

where

E_{impact} = impact energy, $\text{kg} \cdot \text{m}^2/\text{s}^2$

N = number of drops to cause ultimate crack

m = mass of drop weight, kg

g = gravitational acceleration, m/s^2

h = height of drop weight, m



Figure 3.32: Repeated Drop Weight Impact Test.

3.11 Scanning Electron Microscope and Energy Dispersive X-ray Analysis

Scanning Electron Microscope (SEM) and Energy Dispersive X-ray (EDX) analysis were used to characterise the concrete's surface. Both of the analyses were performed in compliance with ASTM C1723 (2016).

3.11.1 Scanning Electron Microscope (SEM)

A SEM was used to analyse the microstructure of hardened concrete (Frýbort, Štulířová and Grošek, 2020). According to ASTM C1723 (2016), SEM has been used to examine concrete since the 1960s and has shown to be an effective method for the microstructural analysis of concrete. The operating mechanism of the SEM is based on the penetration of electron beams into the surface of the object. After that, the surface image is produced by the releasing electrons and photons.

SEM was performed on the fracture surfaces of the concrete sample after the compression tests. The diameter and height of the concrete sample should not be larger than 15 mm and less than 40 mm, respectively. Since the concrete is a non-conductive material, so the sample should be coated with a thin layer of gold by using the sputter coater machine as shown in Figure 3.33. After the surface of the concrete samples were conductive, the samples were placed in the vacuum chamber of the SEM machine as shown in Figure 3.34. The concrete sample was scanned for both normal and back scattered scanning. The image magnification of 50 \times , 100 \times , 200 \times , 500 \times and 1000 \times were observed for the concrete sample.

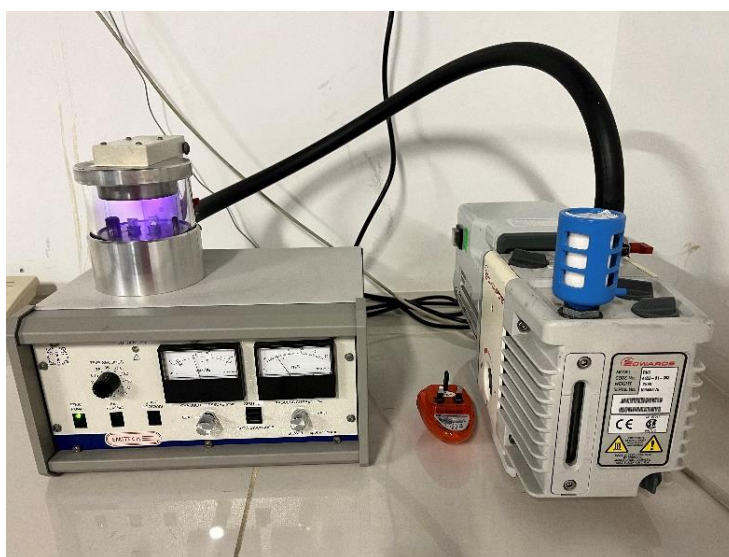


Figure 3.33: Coating of Specimens in Sputter Coater Machine.



Figure 3.34: Specimens Were Placed in Vacuum Chamber.

3.11.2 Energy Dispersive X-ray (EDX)

EDX is to give fundamental quantitative information on the composition of material elements in hardened concrete. For example, the elements such as Calcium (Ca), Oxygen (O), Aluminum (Al), Silicon (Si), Magnesium (Mg) and Sulphur (S). The probe for the EDX analysis is common equipment with the SEM machine, which is Hitachi VP-SEM S-3700N as shown in Figure 3.35. According to ASTM C1723 (2016), the compositional results can be associated with specific features visible in the SEM image. The operating mechanism of the EDX is to remove the inner shell electrons by bombarding the sample surface with high-energy electron beams. Then, the removed electrons are then replaced by outer shell electrons, resulting in particular X-ray wavelengths depending on the atomic structure of the elements (Ebnesajjad, 2011). As a result, the composition of the element in the sample is analysed.



Figure 3.35: Hitachi VP-SEM S-3700N.

3.12 Summary

In this chapter, the complete process of the study, from the preparation of the raw material and mixing procedures to the testing method were discussed. The material needed includes Ordinary Portland Cement (OPC), coarse and fine aggregate, water, superplasticizer, crumb rubber, Styrene-Butadiene (SBR) Latex, silica fume and steel fiber. Latex based rubberized concrete (LRC) and latex based rubberized concrete with 15 kg/m^3 steel fiber (LRC-15 % SF) were produced. The mix proportions for various mixes (LRC and LRC-15 % SF) were prepared. Both trial mixes with the W/C ratios of 0.28, 0.30 and 0.32 were needed to proceed to reach the 28 days cubic compressive strength of 55 MPa. The optimum combination of the trial mix for both LRC and LRC-15 % SF had achieved at least 55 MPa of 28 days characteristic strength and was selected for testing.

Cubic, cylindrical and prism specimens of LRC and LRC-15 % SF were cast to carry out the hardened destructive test. Seventy-two concrete specimens were needed to be prepared. The cubic specimen was used for the compressive and repeated drop weight impact tests. Cylindrical and prism

specimens were utilised for splitting tensile and flexural tests, respectively. The curing age of each test specimen should vary from 7 days, 28 days and 56 days. 1 hour of oven dried is required for all testing specimens before testing. All the mixing and testing procedures and testing in this study follow BS and ASTM standards. SEM and EDX analyses were performed in compliance with ASTM C1723 (2016).

CHAPTER 4

TRIAL MIX

4.1 Introduction

This chapter presents tensile testing for steel fiber and discusses the mix proportion, fresh properties and compressive strength of the latex based rubberized concrete (LRC) and latex based rubberized concrete with 15 kg/m^3 steel fiber (LRC-15 % SF) with the W/C ratio 0.28, 0.30 and 0.32. Based on the obtained results, the optimal mixture of LRC and LRC-15% SF was chosen for further testing of the experimental work, which focuses primarily on the compressive, splitting tensile and flexural strengths, as well as the impact resistance of the various specimens.

4.2 Tensile Testing for Steel Fiber

A tensile test was conducted in accordance with ASTM A370 (2022) to determine the mechanical properties of steel fiber and their potential for reinforcing the concrete. The results of the tensile test for steel fiber are summarised in Table 4.1.

The average tensile stress at a yield offset of 0.2 % was 33.45 MPa. This value also called the yield strength or yield point, which represents the stress at which the steel fiber begins to deform permanently. Next, the steel fiber had an ultimate tensile strength and ultimate load of 1423.19 MPa, and 338.13 N, respectively, representing the maximum stress and maximum load the steel fiber can withstand before it fails. Besides, Figure 4.1 illustrates the stress-strain curve for steel fiber.

Table 4.1: Tensile Test Results for Steel Fiber.

Avg. Tensile Stress at Yield Offset 0.2 % (MPa)	Avg. Maximum Tensile Stress (MPa)	Avg. Load at Maximum Tensile Stress (N)	Strain at Maximum Stress (%)
33.45	1423.19	338.13	11.15

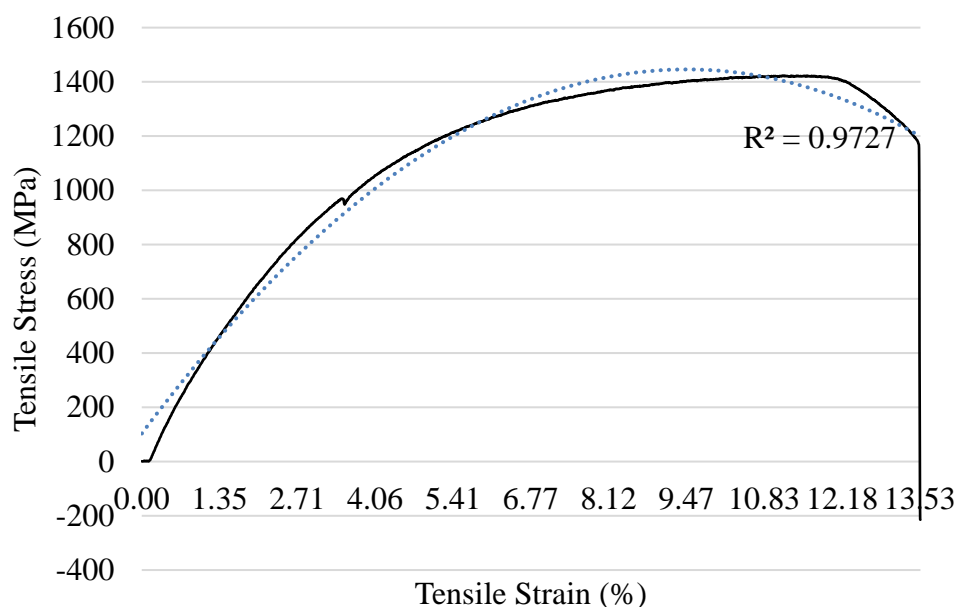


Figure 4.1: Stress-Strain Curve for Steel Fiber.

4.3 Control Mix

The materials used for the control mix of latex based rubberized concrete (LRC-CTR) included: Ordinary Portland Cement (OPC), water, superplasticizer, fine aggregates, coarse aggregates, rubber granules, SBR latex and silica fume. Table 4.2 shows the mix proportion design for the trial mix of latex based rubberized concrete with the W/C ratio 0.28, 0.30 and 0.32. In all of the design mix, 11.7 % of the volume of sand was substituted with crumb rubber, 3 % of SBR latex was incorporated based on the weight of cement and the silica fume replaced part of the cement content. In addition, the dosage of superplasticizer varied from 1.00 % to 1.20 % by weight of cement depending on the quantity of water used for each design concrete mix.

Table 4.2: Mix Proportions of Trial Mixes for LRC-CTR.

W/C	Unit Weight (kg/m ³)								
	Cement	Aggregate			Crumb Rubber	SBR Latex	Silica Fume	SP	SF
		Fine	20 mm	10 mm					
0.32	667	362	738	369	20	20	40	6.67	0
0.30	667	362	738	369	20	20	40	7.34	0
0.28	667	362	738	369	20	20	40	8.00	0

Note:

The mix proportions are based on 1 m³ concrete volume using the absolute method.

4.3.1 Fresh Properties

The workability of the fresh concrete was assessed through the implementation of the slump test and compacting factor test. The slump value and compacting factor against different design mixes are shown in Figure 4.2.

A decrease in the W/C ratio results in a reduction in the workability of the concrete mixture, making it more challenging to handle and place. However, there is a solution to this problem. Increasing the dosage of superplasticizer in the lower W/C ratio mix design makes it possible to maintain the workability of the mixture while still achieving a lower W/C ratio. In this research, the dosage of superplasticizer was 1.00 %, 1.10 % and 1.20 % when the W/C ratio was reduced from 0.32 to 0.28 with an interval of 0.02. Thus, from Figure 4.2, the slump value and compacting factor for all the design mixes were consistent. Therefore, using the right amount of superplasticizer can achieve a lower W/C ratio without sacrificing the workability of the fresh concrete.

In terms of the compacting factor, the results obtained in all the design mixes were between 0.90 to 0.95, which falls in the range of the desired value (0.80 - 1.00). In short, the fresh concrete can flow and fill all the spaces within the formwork without segregation or bleeding.

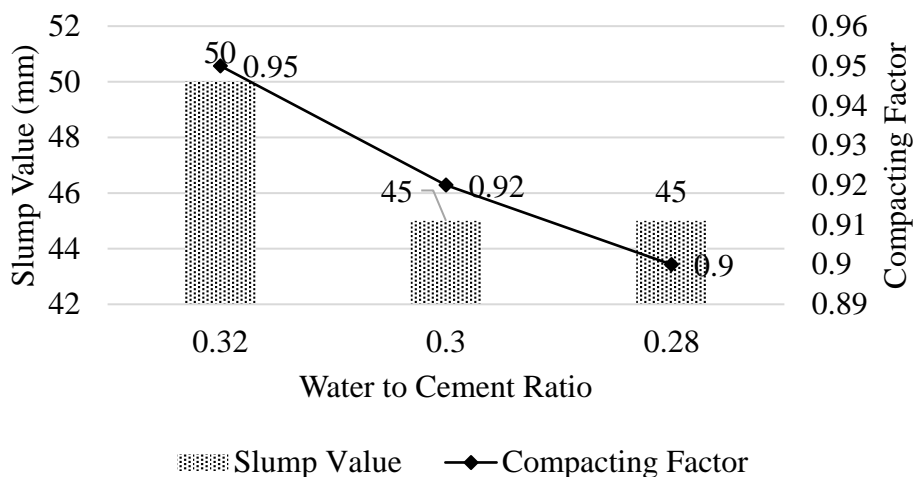


Figure 4.2: Fresh Properties of Trial Mixes for LRC-CTR.

4.3.2 Density

In this study, there were two types of density obtained through the experiment, which were fresh density and hardened density. Figure 4.3 shows the fresh and hardened density against the various design mix proportion. Based on the result, the fresh and hardened density increased when the W/C ratio decreased. The decreased in hardened density compared to fresh density may be attributed to the process of hydration. As the concrete hardens and undergoes the process of hydration, some small voids and pores will form within the concrete, which can reduce the overall density.

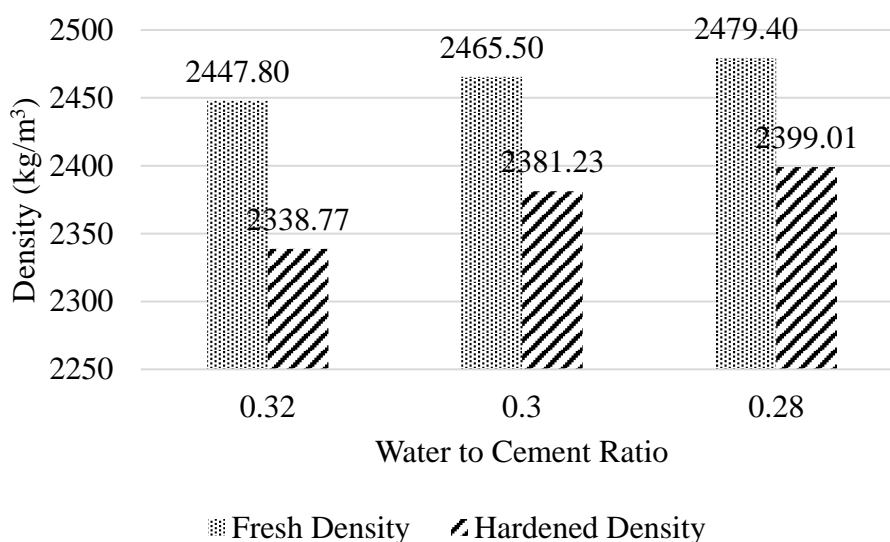


Figure 4.3: Density of Trial Mixes for LRC-CTR.

4.3.3 Compressive Strength

The trial mix of cubic specimens for LRC were prepared and cured for 7 days and 28 days. Appendix A-4 shows compressive test results for the trial mixes of LRC-CTR. Then, the optimum combination of the trial mix, which had achieved at least 55 MPa of 28 days characteristic strength, was chosen to test for the splitting tensile and flexural strengths, as well as impact resistance in this study. Figure 4.4 shows the compressive strength of LRC-CTR with various W/C ratios.

Because both LRC-CTR with the W/C ratios of 0.32 and 0.30 could not achieve the desired strength at 28 days, other changes must be made, such as reducing the W/C ratio or increasing the cement content. The concluding water-to-cement ratio (W/C) in this research was established as 0.28. The design mix (LRC-CTR 0.28) has a compressive strength of 56.62 MPa on the 28th day. In short, LRC-CTR with the W/C of 0.28 was chosen for further testing on the splitting tensile and flexural strengths, as well as impact resistance.

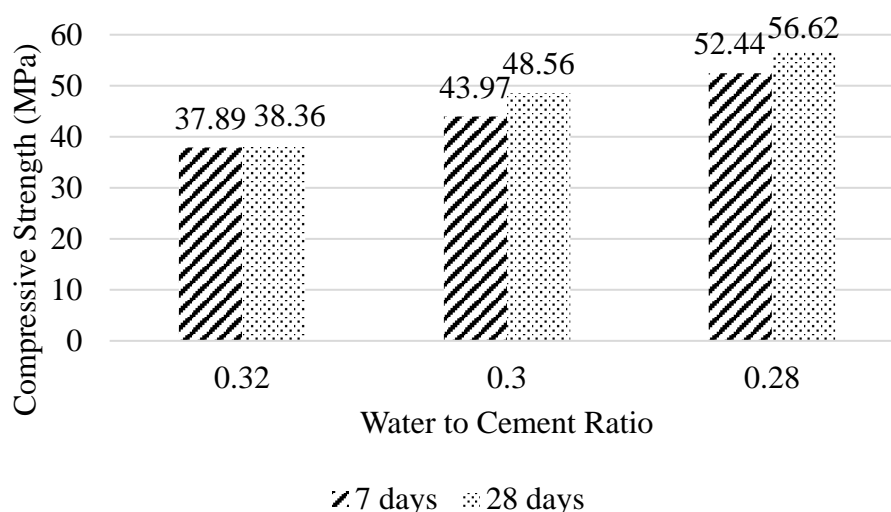


Figure 4.4: Compressive Strength of Trial Mixes for LRC-CTR.

4.4 Steel Fiber Mix

Ordinary Portland Cement (OPC), water, superplasticizer, fine aggregates, coarse aggregates, crumb rubber, SBR Latex, silica fume and steel fiber were incorporated into the control mix of LRC-15 % SF. The design mix proportion of the trial mix for LRC-15 % SF with W/C ratios of 0.28, 0.30, and 0.32 are

shown in Table 4.3. In the entire design mix, crumb rubber replaced 11.7 % of the volume of sand, 3 % of SBR latex was incorporated based on the weight of cement, and silica fume replaced a portion of the cement content. Besides, the superplasticizer dosage varied between 1.10 % and 1.25 % by weight of cement, depending on the quantity of water used in each concrete mix design.

Table 4.3: Mix Proportions of Trial Mixes for LRC-15 % SF.

W/C	Unit Weight (kg/m ³)								
	Cement	Aggregate			Crumb Rubber	SBR Latex	Silica Fume	SP	SF
		Fine	20 mm	10 mm					
0.32	667	362	738	369	20	20	40	7.34	15
0.30	667	362	738	369	20	20	40	8.00	15
0.28	667	362	738	369	20	20	40	8.34	15

Note:

The mix proportions are based on 1 m³ concrete volume using the absolute method.

4.4.1 Fresh Properties

Figure 4.5 illustrates the slump value and compacting factor for various design mixtures. In the lower water-to-cement ratio mix design, the superplasticizer can be increased to maintain workability. In this study, the superplasticizer dosage was 1.10 %, 1.20 %, and 1.25 %, as the W/C ratio decreased from 0.32 to 0.28 with a 0.02 interval. The slump values were consistent with each other among all the design mixes. This has definitely proved that the usage of superplasticizers has increased the workability of fresh concrete in a lower W/C ratio. The obtained values for the compacting factor, namely 0.91, 0.86, and 0.94, fell within the targeted range of 0.80 to 1.00.

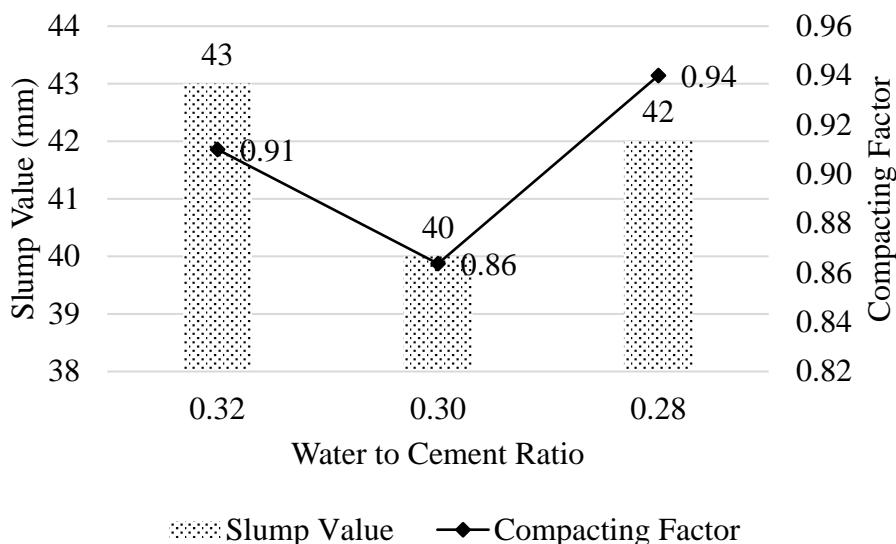


Figure 4.5: Fresh Properties of Trial Mixes for LRC-15 % SF.

4.4.2 Density

The fresh and hardened density for LRC-15 % SF with W/C ratios of 0.28, 0.30, and 0.32 are illustrated in Figure 4.6. Similar to the control mix (LRC-CTR), the fresh and hardened density increased when the W/C ratio was reduced. However, the increment was not significant. It was found that the hardened density was a little bit lower than the fresh density, with LRC-15 % SF 0.30 having the largest percentage discrepancy reported at 6.3 %.

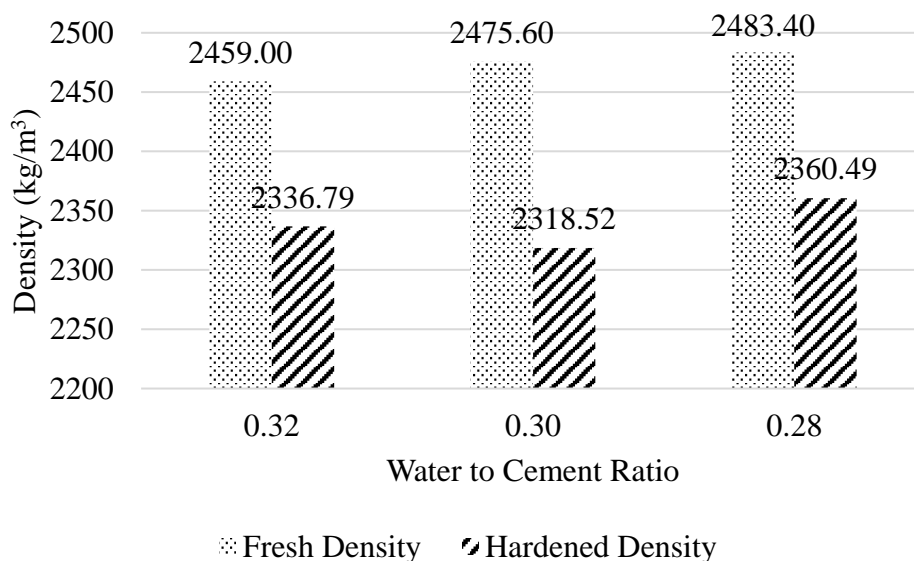


Figure 4.6: Density of Trial Mixes for LRC-15 % SF.

4.4.3 Compressive Strength

Eighteen cubic specimens for the LRC were prepared and cured for 7 and 28 days. Appendix A-5 shows compressive test results for the trial mixes of LRC-15 % SF. In this study, the splitting tensile and flexural strengths, as well as impact resistance of LRC-15 % SF were evaluated using the optimal combination of the trial mix, which had achieved at least 55 MPa of 28 day characteristic strength. Figure 4.7 illustrates the compressive strength of LRC-15 % SF with varying ratios of water to cement.

Due to the fact that LRC-15 % SF 0.32 did not achieve the desired strength at 28 days, other modifications, such as decreasing the W/C ratio, have been made. When the W/C ratio was adjusted to 0.30 and 0.28, the compressive strength increased to 59.47 MPa and 60.89 MPa, respectively, which exceeded the desired strength of 55 MPa. Consequently, the LRC-15 % SF with the W/C ratio of 0.25 and higher strength was chosen for further testing of its splitting tensile and flexural strengths, as well as impact resistance.

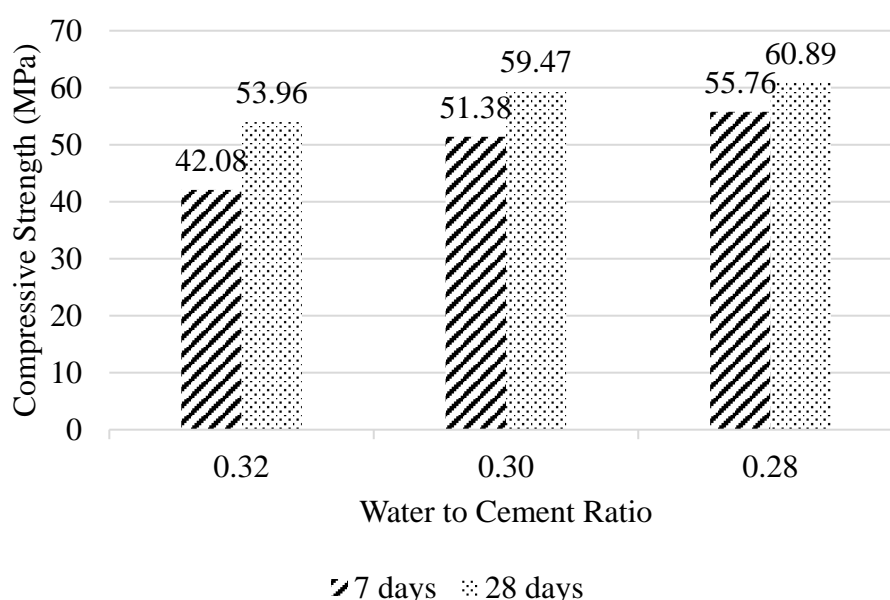


Figure 4.7: Compressive Strength of Trial Mixes for LRC-15 % SF.

4.5 Summary

In short, the tensile test for steel fiber was performed to determine the mechanical properties of steel fiber. Among the trial mixes, LRC-CTR and

LRC-15 % SF with the W/C of 0.28, which have achieved the minimum 28 days compressive strength of 55 MPa, were chosen as the optimal mix proportions. The optimum design mix proportions were adopted for further testing of the experimental work, which focuses primarily on the compressive, splitting tensile and flexural strengths, as well as impact resistance.

CHAPTER 5

RESULTS AND DISCUSSION

5.1 Introduction

This chapter examines the effect of incorporating steel fibers in the latex based rubberized concrete in terms of compressive, splitting tensile, flexural strengths, as well as impact resistance. Besides, the morphology and elemental composition of hardened cement paste in LRC-CTR and LRC-15 % SF have also been discussed. The specimens of LRC-CTR and LRC-15 % SF were cured for 7, 28 and 56 days prior to testing.

5.2 Real Mix Proportions

Ordinary Portland Cement (OPC), water, superplasticizer, fine aggregates, coarse aggregates, rubber granules, SBR Latex, and silica fume were used in the LRC-CTR and LRC-15 % SF. However, 15 kg/m³ of steel fiber was added to the design mix of LRC-15 % SF. The W/C ratios for both design mixes were set at 0.28. The dosage of superplasticizer for LRC-CTR and LRC-15 % SF was 1.20 % by weight of cement, respectively. The design mix proportions for LRC-CTR and LRC-15 % SF are tabulated in Table 5.1.

Table 5.1: Design Mix Proportions of LRC-CTR and LRC-15 % SF.

Design Mix	W/C	Unit Weight (kg/m ³)								
		Cement	Aggregate			Crumb Rubber	SBR Latex	Silica Fume	SP	SF
			Fine	20 mm	10 mm					
LRC-CTR	0.28	667	362	738	369	20	20	40	8.00	0
LRC-15 %SF	0.28	667	362	738	369	20	20	40	8.00	15

Note:

The mix proportions are based on 1 m³ concrete volume using the absolute method.

5.3 Fresh Properties

The fresh properties such as slump value and compacting factor of LRC-CTR and LRC-15 % SF are illustrated in Figure 5.1.

Figure 5.1 indicates that the addition of 15 kg/m³ of steel fiber reduced the slump by 7 % compared to the control mixture. It was anticipated that the use of steel fibers would reduce slump. Similar to the results of Alsaif and Alharbi (2022), the experiment concluded that due to the presence of steel fibers, the internal friction between concrete components was increased. In addition, the steel fibers agglomerated, restricting the aggregate's free mobility and thus, decreasing the workability of the fresh concrete. Besides, the compacting factor was also reduced when the steel fiber was added. This may be owing to the greater specific surface area resulting from higher fiber content. In addition, the steel fibers were dispersed in a non-uniform manner within the matrix, restricting the flow of fresh concrete.

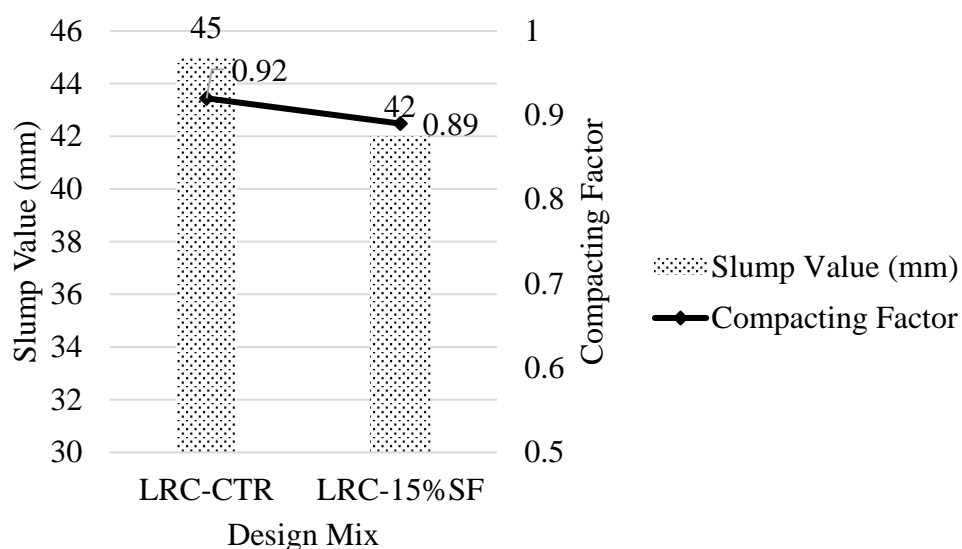


Figure 5.1: Fresh Properties of LRC-CTR and LRC-15 % SF.

5.4 Density

There were two types of density, namely, fresh density and hardened density were obtained through the experiment of the real mix. Figure 5.2 shows the fresh and hardened density of LRC-CTR and LRC-15 % SF.

From Figure 5.2, it was discovered that the addition of steel fibers does not result in a notable rise in fresh density and hardened density. The obtained results are similar and with no more than 1 % differences. Similar results were obtained with Chajec and Sadowski (2020). The slight difference in density of LRC-15 % SF is attributed to the relatively low weight of the fibers when compared with the weight of concrete, as the weight of fibers is less than 1 % of the weight of concrete.

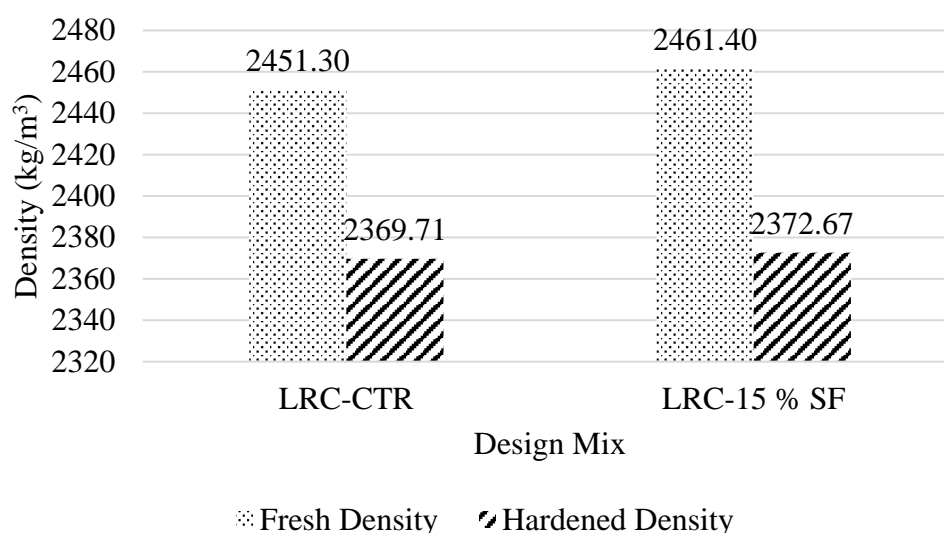


Figure 5.2: Density of LRC-CTR and LRC-15 % SF.

5.5 Hardened Properties

The compressive, splitting tensile, flexural and repeated drop weight impact tests were performed in this study. The results of compressive strength, splitting tensile strength and flexural strength tests are tabulated in Appendix A-6, Appendix A-7 and Appendix A-8, respectively.

5.5.1 Compressive Strength

The compressive strength of LRC-CTR and LRC-15 % SF for 7 days, 28 days and 56 days curing ages are shown in Figure 5.3. It can be observed that the compressive strength of both LRC-CTR and LRC-15 % SF increased as the curing age progressed.

Besides, the addition of steel fibers in the mix has resulted in higher compressive strength at all curing ages compared to the LRC-CTR mix. A

similar result can also be obtained from the work of Eisa, Elshazli and Nawar (2020). The researchers claimed that the maximum compressive strength would be raised might be due to the fact that steel fibers would bridge micro-cracks at an early age and then limit crack formation. The compressive strength of LRC-15 % SF was 8.96 % higher than LRC-CTR at 7 days. This can be attributed to the early strength gain resulting from the incorporation of steel fibers into the mix, which accelerated the hydration process and improved the interlocking of the concrete matrix. Besides, at 28 days, the compressive strength of LRC-15 % SF was 5.36 % higher than LRC-CTR. This can be attributed to the continuing hydration process facilitated by the improved matrix structure resulting from the incorporation of steel fibers. At 56 days, the compressive strength of LRC-15 % SF was 3.18 % higher than LRC-CTR due to the slower rate of strength gain at the later age. In short, the incorporation of steel fibers into the concrete mix enhanced its strength characteristics, especially during the early stages of curing.

In terms of the curing period, the finding indicated that the percentage rising in compressive strength for LRC-CTR and LRC-15 % SF was higher from 7 days to 28 days compared to 28 days to 56 days. The compressive strength of LRC-CTR increased by 17.59 % from 7 days to 28 days, while it only increased by 3.66 % from 28 days to 56 days. Similar to LRC-15 % SF, the compressive strength increased by 13.67 % from 7 days to 28 days, while it only increased by 1.50 % from 28 days to 56 days. During the early stages of curing, the hydration process might be more active, and as a result, the strength gain is more significant. During the curing process, there is a gradual decrease in the rate of hydration, which leads to a slowing down of the strength gain. This might explain why the percentage increase in compressive strength is higher from 7 days to 28 days compared to 28 days to 56 days.

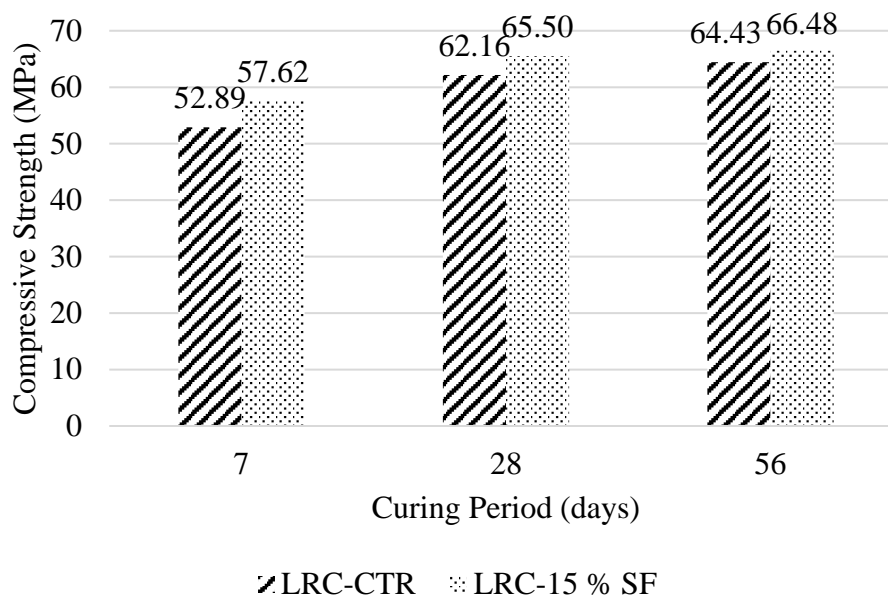


Figure 5.3: Compressive Strength of LRC-CTR and LRC-15 % SF.

5.5.2 Splitting Tensile Strength

The splitting tensile strength of LRC-CTR and LRC-15 % SF for 7, 28 and 56 days of curing ages are shown in Figure 5.4. The results indicated that both types of concrete exhibited a rise in splitting tensile strength as the curing time progressed. For LRC-CTR, the splitting tensile strength increased from 12.44 MPa at 7 days to 14.57 MPa at 28 days and further increased to 18.70 MPa at 56 days. This suggests that the tensile strength of LRC-CTR continues to increase over time as the curing period increases. For LRC-15 % SF, the splitting tensile strength was higher than LRC-CTR at all curing periods. The splitting tensile strength of LRC-15 % SF was observed to be 14.78 MPa at 7 days, which exhibited an increase to 17.03 MPa at 28 days and further increased to 20.70 MPa at 56 days. This suggests that the inclusion of steel fibers in the concrete mixture resulted in an enhancement of the concrete's splitting tensile strength.

At all curing periods, the splitting tensile strength of LRC-15 % SF exhibited better performance in comparison to that of LRC-CTR. The increase in splitting tensile strength for LRC-15 % SF compared to LRC-CTR was found to be 18.80 % at 7 days, 16.89 % at 28 days, and 10.70 % at 56 days. A similar phenomenon can be observed in the finding of Eisa, Elshazli and Nawar (2020). In the experiment, the splitting tensile test was conducted by

adding steel fibers to the rubberized concrete. The experimental results showed that adding steel fibers to concrete helps to bridge microcracks and boost the tensile strength at an early stage. The steel fiber has high tensile strength, which helps to reinforce the concrete and prevent cracks from forming. Therefore, this indicates that the addition of steel fibers has a positive effect on the splitting tensile strength and can improve the suitability for structural applications.

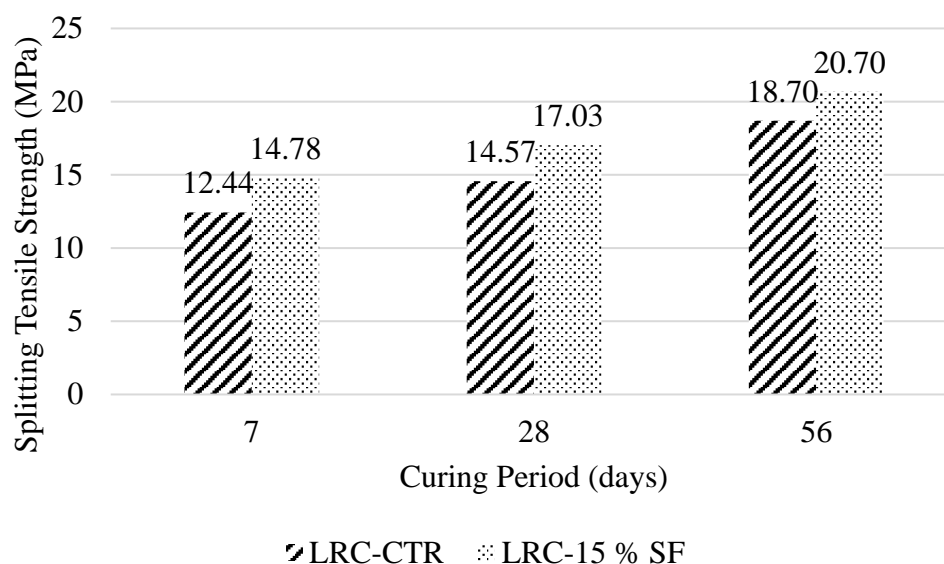


Figure 5.4: Splitting Tensile Strength of LRC-CTR and LRC-15 % SF.

Figure 5.5 shows the splitting tensile / compressive strength ratio of LRC-CTR and LRC-15 % SF at 7, 28 and 56 days. The inclusion of steel fibers resulted in an increase in the split tensile/compressive strength ratio for LRC, as observed. This might be due to the incorporation of steel fibers in LRC enhancing its tensile strength.

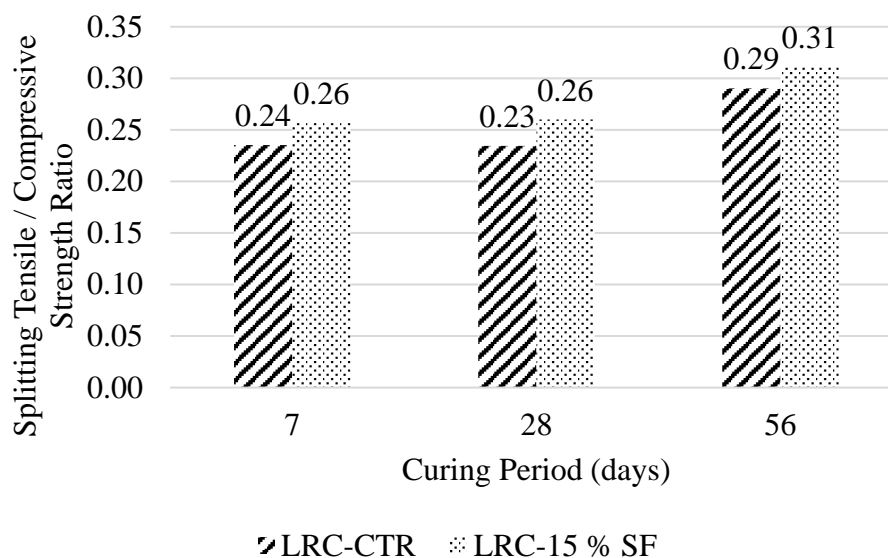


Figure 5.5: Splitting Tensile/ Compressive Strength Ratio.

5.5.3 Flexural Strength

The flexural strength of LRC-CTR and LRC-15 % SF for 7 days, 28 days and 56 days curing ages are shown in Figure 5.6.

From Figure 5.6, LRC-15 % SF has shown higher flexural strength compared to LRC-CTR at all curing periods. This phenomenon is expected since the reinforcing effect of steel fibers, which act as a bridge between the cracks, prevent them from propagating further and enhances the load-bearing capacity of the concrete. At 7 days, the flexural strength of LRC-15 % SF is 16.16 % higher than that of LRC-CTR. This percentage increased to 24.19 % at 28 days and 17.94 % at 56 days. The data indicates that the increase in flexural strength was highest at 28 days for both LRC-CTR and LRC-15 % SF. This might be due to the presence of steel fiber in the LRC mixture has led to an increase in the flexural strength over time.

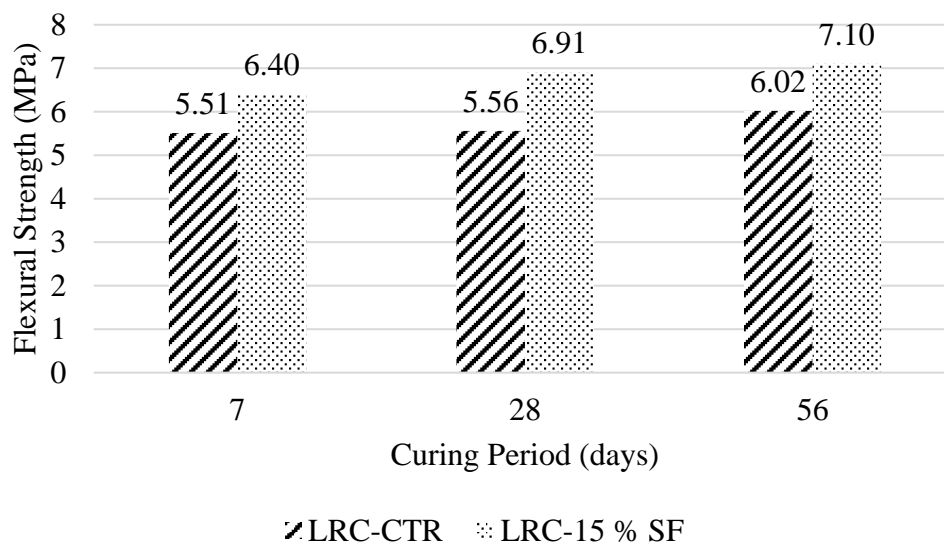


Figure 5.6: Flexural Strength of LRC-CTR and LRC-15 % SF.

Figure 5.7 shows the flexural strength / compressive strength ratio of LRC-CTR and LRC-15 % SF at 7, 28 and 56 days. In terms of flexural/compressive strength ratio, LRC with the inclusion of steel fibers had a generally higher ratio at all curing periods. However, the ratio did not show much difference as compared to LRC. The increase in the ratio was observed to be only 0.01, 0.02, and 0.02 at 7, 28, and 56 days of curing, respectively.

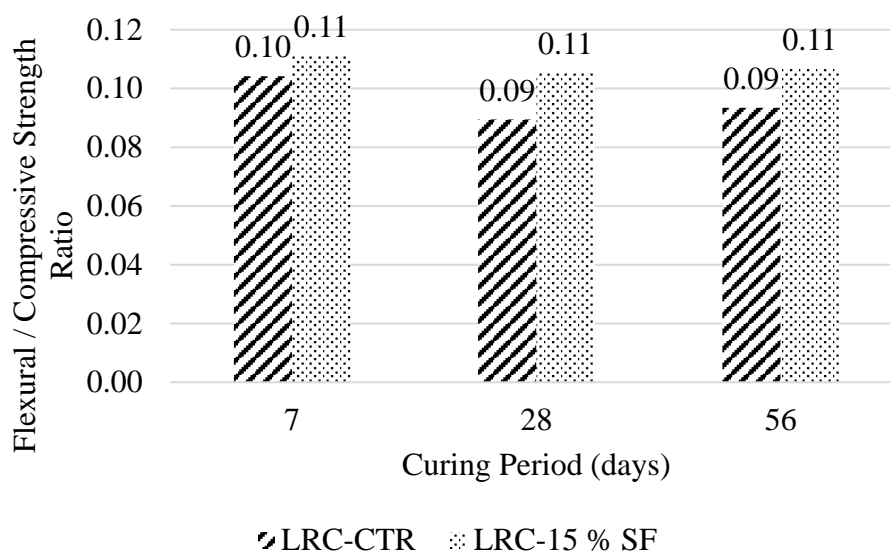


Figure 5.7: Flexural / Compressive Strength Ratio.

Besides, Figure 5.8 and Figure 5.9 show the flexural failure pattern of LRC-CTR and LRC-15 % SF, respectively. It can be observed that the incorporation of steel fibers into the latex rubberized concrete enhances its flexural strength, which means it is less likely to break into two parts during the flexural test. However, the LRC-CTR break into two part at the end of the test. Steel fibers act as a reinforcement material that might help to distribute the stress applied to the concrete more evenly, which prevents the propagation of cracks under the applied load. Besides, the hooked-end configuration of steel fiber which serves to hold the two part, thereby limiting the occurrence of concrete specimen fragmentation (Hafiz Ahmad and Awang, 2012). On the other hand, LRC-CTR without steel fibers might be more brittle, which means it is more susceptible to cracking and breaking into two parts under the applied load during the flexural test.



Figure 5.8: Flexural Failure of LRC-CTR.



Figure 5.9: Flexural Failure of LRC-15 % SF.

5.5.4 Impact Resistance

Table 5.2 tabulates the experimental result of the impact resistance test for both span lengths of 400 mm and 200 mm. Based on Table 5.2, it appears that LRC-15 % SF performed better than the LRC-CTR in terms of impact resistance, as demonstrated by the higher number of drops required to cause ultimate failure.

In both span lengths of 400 mm and 200 mm impact tests, the average number of drops required to cause ultimate failure for LRC-15 % SF was higher than LRC-CTR in all curing periods. For the tested span length of 400 mm, the number of drops required to cause ultimate failure increased with curing age. Besides, the results show that the span length impacted the number of drops required to cause ultimate failure. In both LRC-CTR and LRC-15 % SF, the average number of drops required to cause ultimate failure was higher for the shorter span length of 200 mm compared to the longer span length of 400mm. This could be due to the increased rigidity and stiffness of the shorter span length, making it more difficult for the materials to deform and ultimately fail.

Table 5.2: Experimental Result of Impact Resistance Test.

Design Mix	Average No. of drops		
	7 days	28 days	56 days
LRC-CTR (400 mm)	6.67	21.00	31.00
LRC-CTR (200 mm)	25.00	30.67	45.33
LRC-15 %SF (400 mm)	20.33	38.33	45.33
LRC-15 %SF (200 mm)	40.67	48.67	52.00

For a more accurate evaluation on impact resistance, the impact energy absorbed in Joules should be compared. This is because converting the number of blows to the absorbed energy would allow for a more accurate comparison of all specimens. Thus, the impact resistance of LRC-CTR and LRC-15 % SF for 7 days, 28 days and 56 days curing ages are shown in Figure 5.10.

The impact energy absorbed by the LRC-15 % SF was 205.34 % higher than the LRC-CTR at 7 days, 82.55 % higher at 28 days, and 46.27 % higher at 56 days in a span length of 400 mm. Similarly, in the 200 mm span length, the impact energy absorbed by the LRC-15 % SF was 62.97 % higher than the LRC-CTR at 7 days, 58.53 % higher at 28 days, and 14.71 % higher at 56 days. These results demonstrated that the presence of steel fibers in the LRC significantly enhances its impact energy absorption capacity, resulting in a much higher percentage increase in the impact energy absorbed compared to the latex based rubberized concrete without steel fibers. This result is consistent with what was noted in the finding of Ismail and Hassan (2017). The experiment concluded that the presence of steel fibers along a crack effectively improves the stress transfer along this crack, resulting in a significantly greater resistance to crack widening. Consequently, greater impact energy is necessary to impose effective stresses that can break the bond between the fibers and the concrete. This improvement shows that it might be take advantage of the positive interaction between steel fiber and crumb rubber to create types of concrete that could be used in high-impact structural applications.

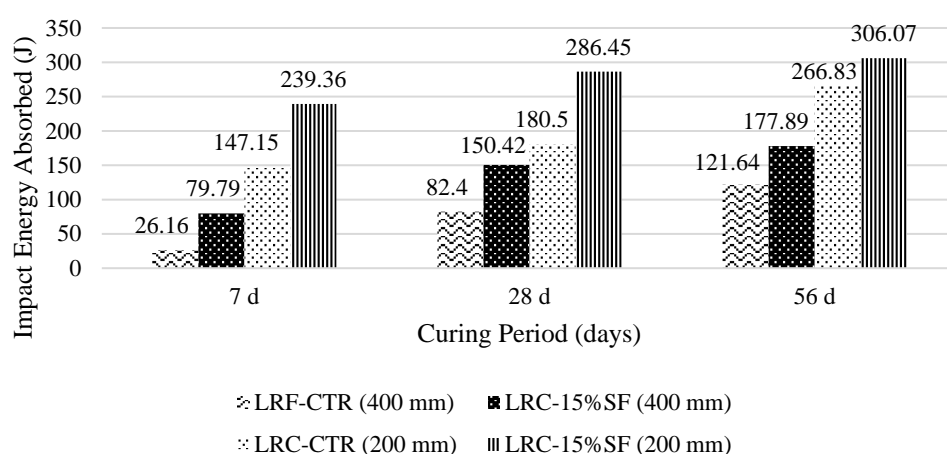


Figure 5.10: Impact Resistance of LRC-CTR and LRC-15 % SF.

In terms of the fracture pattern, both the LRC-CTR and LRC-15 % SF specimens will develop a first crack on the surface of the specimens. However, as the test progressed, the LRC-CTR specimens failed

catastrophically, breaking into two parts when they reached ultimate failure, as shown in Figure 5.11. However, the LRC-15 % SF specimens did not completely fracture into two parts, as shown in Figure 5.12. This is because the steel fibers act as crack arrestors and provide reinforcement to the concrete matrix, resulting in higher toughness and ductility. As a result, the concrete matrix can undergo more deformation and energy absorption under repeated impact loads, leading to less likely to completely fracturing into two parts. In contrast, when subjected to repeated impact loads, the LRC-CTR concrete matrix eventually fractures and fails catastrophically, resulting in two parts. Figure 5.13 shows the LRC-CRT fragment in half in a span length of 200 mm impact test.



Figure 5.11: Fracture Pattern of LRC-CTR.



Figure 5.12: Fracture Pattern of LRC-15 % SF.



Figure 5.13: Fracture Pattern of LRC-CTR (200 mm).

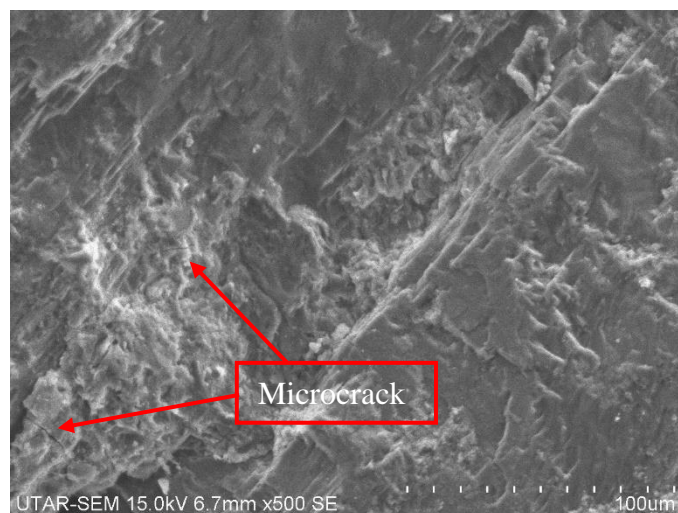
5.6 SEM Morphologies

SEM analysis was conducted to acquire a more comprehensive understanding of the microstructure and morphology of the LRC-CTR and LRC-15 % SF. The microstructure views of LRC-CTR and LRC-15 % SF at 500 \times magnification power are shown in Figure 5.14.

In both LRC-CTR and LRC-15 % SF, a homogeneous and denser microstructure, with no voids was observed. This is mainly due to the presence of SBR latex coated rubber, which acts as a filler or binder, filling in the gaps between the aggregate particles and coating the surface of the particles. However, there were fewer microcracks in the microstructure of LRC-CTR but not in LRC-15 % SF. The incorporation of steel fibers into the LRC can improve tensile strength, preventing the propagation of microcracks. In addition, steel fibers can help to distribute the tensile stresses and prevent the formation and propagation of cracks when the concrete is subjected to external loads. This is because the steel fibers can bridge across the cracks and transfer stresses from one side of the crack to the other.

Besides, it is clear that a strong adhesion exists between the steel fibers and the cement paste, as evidenced by the significant quantity of hydration products adhering to the surface of the steel fibers. There is no doubt that the cement paste, rubber particles and steel fibers form a cohesive structure with the cement paste's dense microstructure.

Moreover, the hydration products are of good quality with no crystallised particles observed. For example, the rod-like crystals of cement hydration product, ettringite (Aft) were not found in both LRC-CTR and LRC-15 % SF.



(a)



(b)

Figure 5.14: SEM Morphology (a) LRC-CTR (b) LRC-15 % SF.

5.7 Elemental Compositions (EDX analysis)

The LRC-CTR and LRC-15 % SF specimens were subjected to EDX analysis in order to determine their existing compound. Besides, in order to acquire a more comprehensive understanding of the inclusion of steel fibers in the LRC, the chemical composition and element distribution were examined. Table 5.3

summarises the weight and atomic percentages of various elements found in the specimens.

Table 5.3: Weight and Atomic Weightage of Element Composition.

Element	LRC-CTR		LRC-15 % SF	
	Weight (%)	Atomic (%)	Weight (%)	Atomic (%)
C	8.24	14.51	6.80	13.27
O	40.63	53.69	31.54	46.25
Mg	0.86	0.75	0.69	0.66
Al	3.41	2.67	3.42	2.97
Si	15.83	11.92	20.81	17.38
S	0.78	0.51	0.46	0.34
Ca	30.26	15.96	23.57	13.79
Fe	-	-	12.72	5.34
Total	100	100	100	100
Ca/Si		1.34		0.80

The Ca/Si ratio in concrete refers to the ratio of the mass of calcium oxide to the mass of silica in the cement used to make the concrete. According to Kjellsen, Wallevik, and Fjällberg (1998), the major hydrated phases in cement paste can be identified by their compositions, which are often characterized by the Ca/Si ratio. The Ca/Si ratio of calcium-silicate-hydrate (C-S-H) is between 0.8 and 2.5, while the Ca/Si ratio of calcium hydroxide (CH) and calcium-aluminate-ferrite-mono (AFm) is greater than or equal to 10 and 4, respectively. Based on Table 5.3, the Ca/Si ratio for both the LRC-CTR and LRC-15 % SF was below 2.5. Thus, indicates that the hydration products are of good quality, mainly CSH, despite the presence of CH, AFm, and other contaminants. Besides, the Ca/Si ratio of LRC-CRT was higher than that of the LRC-15 % SF. According to the study of the Kunther, Ferreiro and Skibsted (2017) compressive strengths of the CSH pastes increased with decreasing Ca/Si ratio. This explains the higher compressive strength of LRC-15 % SF compared to LRC-CTR.

The major existing elements include Carbon (C), Oxygen (O), Magnesium (Mg), Aluminium (Al), Silicon (Si), Sulphur (S) and Calcium (Ca) were observed from the EDX spectrum of LRC-CTR. In this study, the remarkably high carbon content observed for both LRC-CTR and LRC-15 % SF suggested the presence of crumb rubbers in the inspected region. However, an element such as Iron (Fe) was found in LRC-15 % SF due to the inclusion of steel fiber. Figure 5.15 shows the EDX spectrum nearby the steel fiber in LRC-15 % SF. This significant iron peak suggested the presence of steel fiber in the concrete.

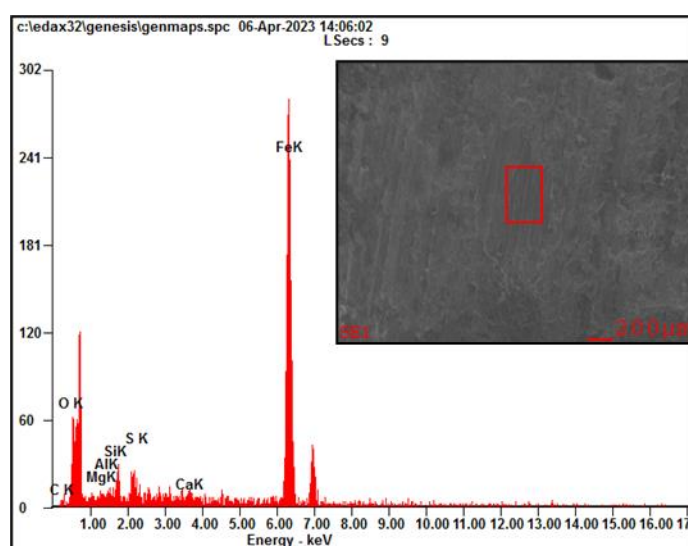


Figure 5.15: EDX Spectrum of LRC-15 % SF.

5.8 Effect of Various Steel Fiber Content on Hardened Properties

The effect of different steel fiber contents (20 kg/m^3 and 25 kg/m^3) inclusion on the hardened properties, namely compressive, splitting tensile and flexural strengths, as well as impact resistance has also been studied in this report.

5.8.1 Compressive Strength

The compressive strength against various mix proportions with different steel fiber contents at all curing ages is illustrated in Figure 5.16. Based on Figure 5.16, the findings indicate that the compressive strength of LRC exhibits an upward trend as the steel fiber content increases, reaching a peak at 20 kg/m^3 . When the quantity of steel fiber inclusion increased from 15 kg/m^3 to 20 kg/m^3 ,

the strength developments increased from 8.9 % to 9.0 %, 4.9 % to 6.2 % and 2.8 % to 11.5 % for the 7, 28 and 56 days of curing, respectively. Wu, et al. (2016) also reported comparable findings. The researchers claimed that an increase in steel fiber content has the potential to reduce the average space between fibers, resulting in a greater number of fiber being able to sustain the load and ultimately leading to the development of multiple cracks. In addition, the stress between the fibers and matrix was observed to decrease as the fiber content increased. This phenomenon led to a delay in the formation and propagation of cracks, ultimately resulting in an increase in strength. However, when the steel fiber content was further increased to 25 kg/m³, there was a decrease in compressive strength for all curing periods. The decrease was more pronounced at the 7 days curing period with a 3.68 % reduction in compressive strength when compared to LRC-20 % SF. According to Raj, et al. (2020), this might be due to the fact that steel fibers induce a balling effect at higher concentrations, resulting in decreased compressive strength. Thus, this suggests that there may be an optimal range of steel fiber content for achieving maximum compressive strength in rubberized concrete.

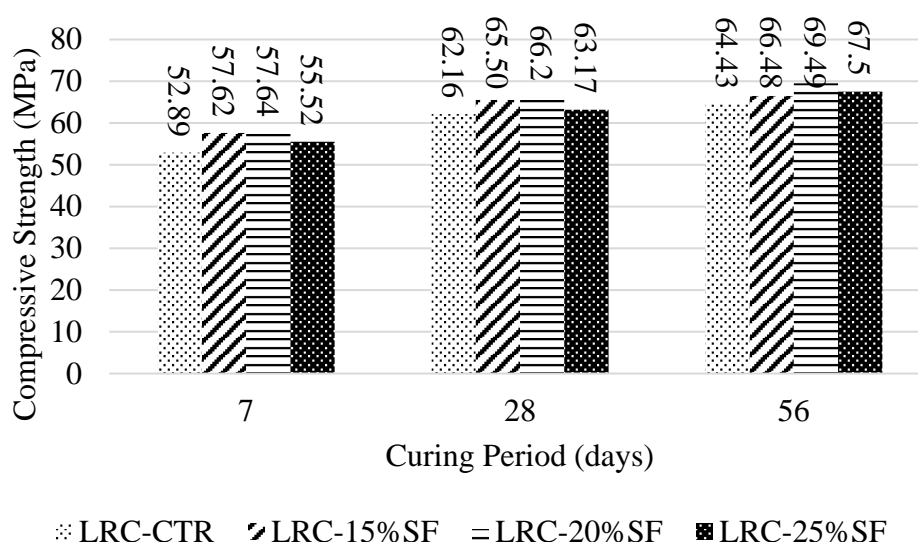


Figure 5.16: Compressive Strength of Various Steel Fiber Design Mixes.

5.8.2 Splitting Tensile Strength

The splitting tensile strength against various mix proportions with different steel fiber contents at all curing ages is illustrated in Figure 5.17. Based on

Figure 5.17, the splitting tensile strength of LRC exhibited an upward trend with an increase in both steel fiber content and curing period. In 28 days of curing, the splitting tensile strength increased from 18.8 % to 43.73 % when the amount of steel fiber inclusion increased from 15 kg/m³ to 25 kg/m³. Besides, LRC-15 % SF appears to have the greatest splitting tensile strength compared to other LRC mixes with various steel fiber contents at 56 days of curing. However, the difference in splitting tensile strength between the other LRC mixes with various steel fiber contents is relatively minor and may not be statistically significant. Further research would be needed to confirm the factors contributing to this trend.

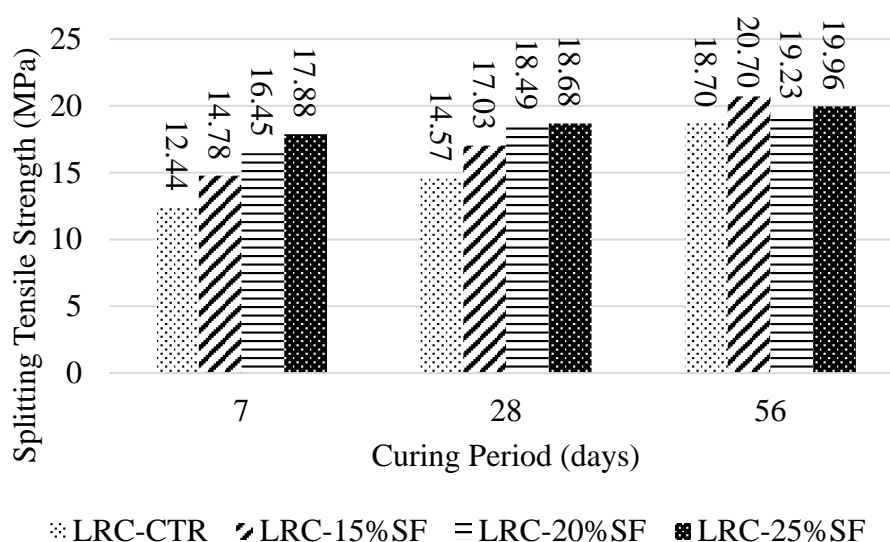


Figure 5.17: Splitting Tensile Strength of Various Steel Fiber Design Mixes.

5.8.3 Flexural Strength

The flexural strength against various mix proportions with different steel fiber contents at all curing ages is illustrated in Figure 5.18. The flexural strength increased by 16.2 %, 47.7 % and 10.5 % at 15 kg/m³, 20 kg/m³ and 25 kg/m³ of steel fiber inclusion, respectively at 7 days of curing age. The flexural strength of LRC-20 % SF is the highest among the others, indicating that the steel fiber content of 20 kg/m³ exerts the most significant impact on early flexural strength. Besides, the results indicate that a greater increment in flexural strength occurred after 28 days of curing. Specifically, the flexural strength increased by 24.3 %, 52.7 %, and 59.7 % for steel fiber inclusions of

15 kg/m³, 20 kg/m³, and 25 kg/m³, respectively. At 56 days of curing, the flexural strength increased by 17.94 %, 45.2 %, and 52.7 %, respectively, for 15 kg/m³, 20 kg/m³, and 25 kg/m³ of steel fiber inclusion. In general, the findings suggest that the incorporation of steel fibers into LRC has the potential to enhance its flexural strength, with a higher steel fiber content leading to higher flexural strength at later curing ages.

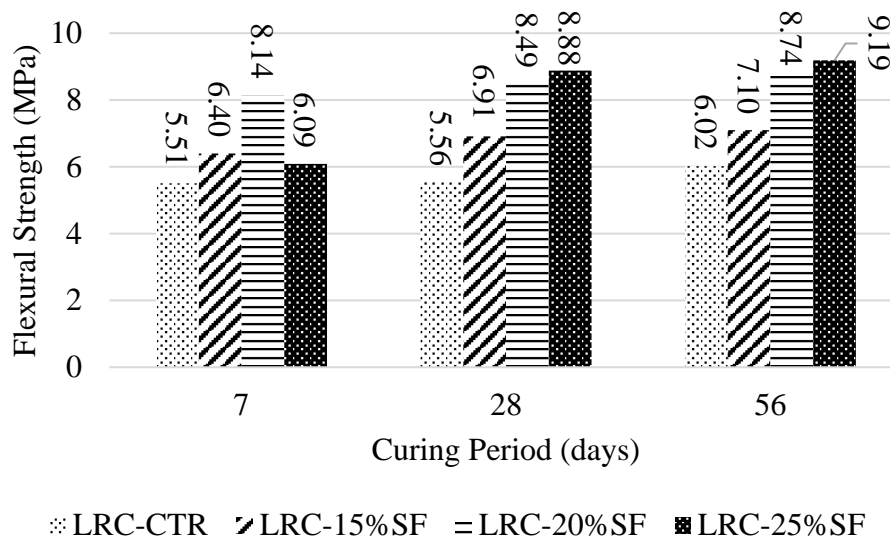


Figure 5.18: Flexural Strength of Various Steel Fiber Design Mixes.

5.8.4 Impact Resistance

Figure 5.19 and Figure 5.20 presents the impact resistance energy against various mix proportions with different steel fiber contents at all curing ages for 400 mm and 200 mm span length, respectively. Based on the results presented, it was evident that the impact resistance energy increased with both the duration of curing and the quantity of steel fiber incorporated into the LRC.

In comparison to the LRC-CTR, LRC-15 % SF and LRC-20 % SF, the LRC-25 % SF showed greater impact resistance energy for both 400 mm and 200 mm span lengths across all curing periods. Specifically, the impact resistance energy increased by 46.2 %, 74.2 % and 91.2 % when 15 kg/m³, 20 kg/m³, and 25 kg/m³ of steel fibers are added into the LRC at 56 days of curing ages, respectively. Besides, the results indicate that the specimens having a span length of 200 mm exhibited a greater impact resistance energy than those with a span length of 400 mm. This trend could be caused by the

shorter span length, which could have made the force at the point of impact more concentrated, causing the specimen to absorb more impact energy. For the LRC-CTR, the impact resistance energy under the 200 mm span length was 119 % higher than that of the 400 mm span length in 56 days. Similarly, for LRC-15 % SF, LRC-20 % SF and LRC-25 % SF, the impact resistance energy 200 mm span length impact test was increased by 72.8 %, 89.9 % and 88.3 %, respectively when compared to the 400 mm span length impact test.

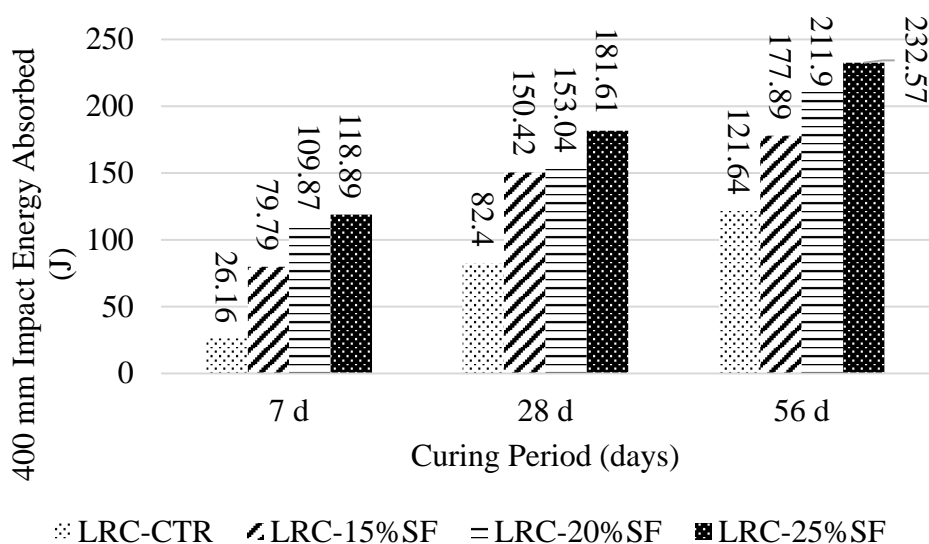


Figure 5.19: Impact Resistance for 400 mm Span Length Impact Test.

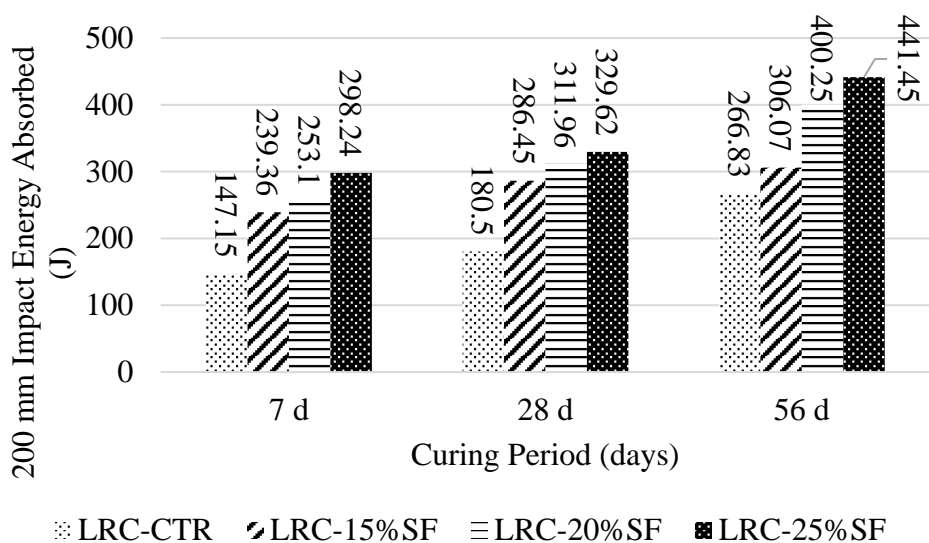


Figure 5.20: Impact Resistance for 200 mm Span Length Impact Test.

5.9 Summary

In short, the addition of steel fibers into LRC reduced the workability but did not result in a notable rise in density. Besides, the inclusion of steel fibers improved the mechanical strength of latex based rubberized concrete due to the role of steel fiber as a reinforcement in the concrete matrix at all curing periods. The compressive, splitting tensile and flexural strengths of both LRC-CRT and LRC-15 % SF were increased with increasing curing periods. Furthermore, the impact energy of LRC-15 % SF is higher than LRC-15 % SF in 7, 28 and 56 days. The fracture pattern of LRC differed from that of LRC-15 % SF, where the specimen of LRC will fragment in half while LRC-15 % SF will only have a crack on the specimen surface. Thus, the inclusion of steel fibers resulted in an enhancement of the impact resistance of the LRC by absorbing energy and reducing the risk of spalling or fragmentation upon impact.

Apart from that, the steel fiber was observed in the morphology of LRC-15 % SF. In view of the elemental compositions study through EDX analysis, the additional element of Iron was found in LRC-15 % SF due to the inclusion of steel fiber.

CHAPTER 6

CONCLUSION AND RECOMMENDATIONS

6.1 Conclusion

After conducting a series of thorough experiments, conclusions pertaining to the objectives outlined at the start of this study are made. The latex based rubberized concrete (LRC) and latex based rubberized concrete with 15 kg/m³ steel fiber (LRC-15 % SF) were produced in cubic, cylinder and prism specimens.

At first, among all the trial mixes, LRC and LRC-15%SF with the W/C of 0.28 was chosen for further fresh and hardened concrete testing since both design mixes met the minimum compressive strength of 55 MPa at 28 days.

Second, steel fiber incorporation reduced the slump value and compacting factor of fresh concrete. The inclusion of steel fiber into LRC resulted in a decrease in its workability. However, the addition of 15 kg/m³ steel fibers did not cause significant changes in the fresh and hardened density.

Third, the hardened properties of LRC-15 % SF were found to be superior to those of LRC-CTR at 7, 28 and 56 days. The compressive strength of LRC-15 % SF was higher than that of LRC-CTR, which indicated that the inclusion of steel fiber improved the strength of the LRC. Similarly, the splitting tensile and flexural strengths of LRC-15 % SF were higher than those of LRC-CTR, indicating that the incorporation of steel fibers into LRC enhanced its toughness and ductility. Moreover, the impact resistance of LRC-15 % SF was higher than that of LRC-CTR, which indicated that the inclusion of steel fiber improved the energy absorption of LRC.

In a nutshell, LRC-15 % SF had achieved the requirement of BS EN 206-1 for the railway sleeper construction with a minimum 28 days compressive strength of 55 MPa. All the results obtained suggest that latex based rubberized concrete with steel fiber can be a suitable material for applications requiring high strength, toughness, and durability. Latex based rubberized concrete with steel fiber might be a good material choice for the

construction of concrete railway sleepers as the railway is exposed to high vibration and impact situations frequently. Furthermore, the incorporation of latex based rubber particles and steel fibers into the concrete mixture can potentially enhance sustainability by employing recycled rubber waste, mitigating environmental problems, and encouraging sustainable construction.

6.2 Recommendations for future work

Based on the findings of this study, latex based rubberized concrete with steel fiber promotes the idea of replacing traditional concrete in the future with a more excellent solution. Several recommendations can be made to improve future research.

- (i) Study the long-term behavior of LRC-15 % SF beyond 56 days of curing as the long-term behavior of concrete is important to assess its durability, and longer curing periods may reveal changes in mechanical strengths.
- (ii) Study the durability of LRC-15 % SF under different environmental conditions such as freeze-thaw cycles, exposure to acidic or alkaline environments, and exposure to aggressive chemicals.
- (iii) Study the structural performance of LRC-15 % SF in structural applications, such as railway sleeper under static and dynamic loading to determine its suitability for structural applications used.
- (iv) Study the effects of different shapes of steel fiber (corrugated, twisted and straight steel fibers) on the properties of latex-based rubberized concrete to optimize the mechanical properties of the LRC.

REFERENCES

Abaza, O.A. and Hussein, Z.S., 2016. Flexural behavior of steel fiber-reinforced rubberized concrete. *Journal of Materials in Civil Engineering*, [e-journal] 28(1). [http://dx.doi.org/10.1061/\(asce\)mt.1943-5533.0001334](http://dx.doi.org/10.1061/(asce)mt.1943-5533.0001334).

Abdelmonem, A., El-Feky, M.S., Nasr, E.-S.A.R. and Kohail, M., 2019. Performance of high strength concrete containing recycled rubber. *Construction and Building Materials*, [e-journal] 227, p.116660. <http://dx.doi.org/10.1016/j.conbuildmat.2019.08.041>.

Abdullah, S.R., Wan Zainal Abidin, W.R. and Shahidan, S., 2016. Strength of concrete containing rubber particle as partial cement replacement. *MATEC Web of Conferences*, [e-journal] 47, p.1009. <http://dx.doi.org/10.1051/mateconf/20164701009>.

Alsaif, A. and Alharbi, Y.R., 2022. Strength, durability and shrinkage behaviours of steel fiber reinforced rubberized concrete. *Construction and Building Materials*, [e-journal] 345, p.128295. <http://dx.doi.org/10.1016/j.conbuildmat.2022.128295>.

American Concrete Institute, 1996. *ACI 544.1R Report on Fiber Reinforced Concrete*. Farmington Hills: American Concrete Institute (ACI).

American Society for Testing and Materials, 2007. *C125 Standard Terminology Relating to Concrete and Concrete Aggregates*. West Conshohocken: ASTM International.

American Society for Testing and Materials, 2007. *C150 Standard Specification for Portland Cement*. West Conshohocken: ASTM International.

American Society for Testing and Materials, 2016. *C1723 Standard Guide for Examination of Hardened Concrete Using Scanning Electron Microscopy*. West Conshohocken: ASTM International.

American Society for Testing and Materials, 2018. *C33/C33M Standard Specification for Concrete Aggregates*. West Conshohocken: ASTM International.

American Society for Testing and Materials, 2018. *D1509 Standard Test Methods for Carbon Black-Heating Loss*. West Conshohocken: ASTM International.

American Society for Testing and Materials, 2018. *D5644 Standard Test Method for Rubber Compounding Materials-Determination of Particle Size Distribution of Recycled Vulcanizate Particulate Rubber*. West Conshohocken: ASTM International.

American Society for Testing and Materials, 2019. *C494/C494M Standard Specification for Chemical Admixtures for Concrete*. West Conshohocken: ASTM International.

American Society for Testing and Materials, 2019. *D5603 Standard Classification for Rubber Compounding Materials—Recycled Vulcanizate Rubber*. West Conshohocken: ASTM International.

American Society for Testing and Materials, 2020. *C1240 Standard Specification for Silica Fume Used in Cementitious Mixtures*. West Conshohocken: ASTM International.

American Society for Testing and Materials, 2020. *C143/C143M Standard Test Method for Slump of Hydraulic-Cement Concrete*. West Conshohocken: ASTM International.

American Society for Testing and Materials, 2022. *A370 Standard Test Methods and Definitions for Mechanical Testing of Steel Products*. West Conshohocken: ASTM International.

American Society for Testing and Materials, 2022. *C1602/C1602M Standard Specification for Mixing Water Used in the Production of Hydraulic Cement Concrete*. West Conshohocken: ASTM International.

American Society for Testing and Materials, 2022. *C31/C31M Standard Practice for Making and Curing Concrete Test Specimens in the Field*. West Conshohocken: ASTM International.

Ansari, S. and Sharma, H., 2017. Comparison of properties of Fiber Mix Reinforced Concrete & Conventional Concrete. *Materials Science, Engineering*, 7(5).

Aslani, F. and Khan, M., 2019. Properties of High-Performance Self-Compacting Rubberized Concrete Exposed to High Temperatures. *Journal of Materials in Civil Engineering*, [e-journal] 31(5), p.4019040. [http://dx.doi.org/10.1061/\(asce\)mt.1943-5533.0002672](http://dx.doi.org/10.1061/(asce)mt.1943-5533.0002672).

Atoyebi, O., Samson O., O., Bello, S. and Cephas, O., 2018. Splitting tensile strength assessment of lightweight foamed concrete reinforced with waste tyre steel fibres. *International Journal of Civil Engineering and Technology*, 9, pp.1129-1137.

Balaha, M. M., Badawy, A. A. M. and Hashish, M., 2007. Effect of using ground waste tire rubber as fine aggregate on the behaviour of concrete mixes. *Indian Journal of Engineering and Materials Sciences*, 14(6).

Behbahani, H. P., Nematollahi, B. and Farasatpour, M., 2011. *Steel Fiber Reinforced Concrete: A Review*. Kandy: ICSECM.

- Bisht, K. and Ramana, P.V., 2017. Evaluation of mechanical and durability properties of crumb rubber concrete. *Construction and Building Materials*, [e-journal] 155, pp.811-817. <http://dx.doi.org/10.1016/j.conbuildmat.2017.08.131>.
- Bordallo, H.N., Aldridge, L.P. and Desmedt, A., 2006. Water dynamics in hardened ordinary Portland cement paste or concrete: from quasielastic neutron scattering. *J Phys Chem B*, [e-journal] 110(36), pp.17966–17976. <http://dx.doi.org/10.1021/jp062922f>.
- British Standards Institution, 2001. *BS EN 206-1 Concrete - Part 1: Specification, performance, production and conformity*. London: BSI.
- British Standards Institution, 2006. *BS EN 14889-1 Fibres for concrete Part 1: Steel fibres Definitions, specifications and conformity*. London: BSI.
- British Standards Institution, 2010. *BS EN 12390-6 Testing hardened concrete Part 6: Tensile splitting strength of test specimens*. London: BSI.
- British Standards Institution, 2019. *BS EN 12350-4 Testing fresh concrete Part 4: Degree of compactability*. London: BSI.
- British Standards Institution, 2019. *BS EN 12390-3 Testing hardened concrete Part 3: Compressive strength of test specimens*. London: BSI.
- British Standards Institution, 2019. *BS EN 12390-5 Testing hardened concrete Part 5: Flexural strength of test specimens*. London: BSI.
- British Standards Institution, 2021. *BS EN 12390-1 Testing hardened concrete Part 1: Shape, dimensions and other requirements for specimens and moulds*. London: BSI.
- Chajec, A. and Sadowski, Ł., 2020. The Effect of Steel and Polypropylene Fibers on the Properties of Horizontally Formed Concrete. *Materials (Basel, Switzerland)*, [e-journal] 13(24), p.5827. <http://dx.doi.org/10.3390/ma13245827>.
- Chandra Gupta, R. and Thomas, B. S., 2016. A comprehensive review on the applications of waste tire rubber in cement concrete. *Renewable and Sustainable Energy Reviews*, [e-journal] 54, pp.1323-1333. <http://dx.doi.org/10.1016/j.rser.2015.10.092>.
- Chanh, N. V., 2015. *Steel Fiber Reinforced Concrete*, Ho Chi Minh: Ho Chi Minh City University of Technology.
- Chemisian Konsultant Sdn.Bhd, 2015. *A study on scrap tyres management for Peninsular*, Kuala Lumpur: National Solid Waste Management Department.

Dehdezi, P.K., Erdem, S. and Blankson, M.A., 2015. Physico-mechanical, microstructural and dynamic properties of newly developed artificial fly ash based lightweight aggregate – Rubber concrete composite. *Composites Part B: Engineering*, [e-journal] 79, pp.451-455. <http://dx.doi.org/10.1016/j.compositesb.2015.05.005>.

Doğan, M. and Bideci, A., 2016. Effect of Styrene Butadiene Copolymer (SBR) admixture on high strength concrete. *Construction and Building Materials*, [e-journal] 112, pp.378-385. <http://dx.doi.org/10.1016/j.conbuildmat.2016.02.204>.

Dong, Q., Huang, B. and Shu, X., 2013. Rubber modified concrete improved by chemically active coating and silane coupling agent. *Construction and Building Materials*, [e-journal] 48, pp.116-123. <http://dx.doi.org/10.1016/j.conbuildmat.2013.06.072>.

Ebnesajjad, S., 2011. Surface and material characterization techniques. In: *Handbook of adhesives and surface preparation*. s.l.:William Andrew Publishing, pp.31-48.

Eisa, A.S., Elshazli, M.T. and Nawar, M.T., 2020. Experimental investigation on the effect of using crumb rubber and steel fibers on the structural behavior of reinforced concrete beams. *Construction and Building Materials*, [e-journal] 252, p.119078. <http://dx.doi.org/10.1016/j.conbuildmat.2020.119078>.

Essa, M. S., Amir, A. M. A. and Hassan, N. F., 2012. Effect of Adding (SBR) on Concrete Properties and Bond Between Old and New Concrete. *Kufa Journal of Engineering*, 4(1), pp.81-95.

Fawzy, H., Mustafa, S. and Elshazly, F., 2020. Rubberized concrete properties and its structural engineering applications – An overview. *The Egyptian International Journal of Engineering Sciences and Technology*, [e-journal] 30, pp.1-11. <http://dx.doi.org/10.21608/eijest.2020.35823.1000>.

Frýbort, A., Štulířová, J. and Grošek, J., 2020. Complementary analyses of concrete characteristics performed on cores taken from concrete pavements. *4th International Scientific Conference Structural and Physical Aspects of Construction Engineering (SPACE 2019)*, 310(36), p.11. <http://dx.doi.org/10.1051/mateconf/202031000036>.

Ganjian, E., Khorami, M. and Maghsoudi, A.A., 2009. Scrap-tyre-rubber replacement for aggregate and filler in concrete. *Constr. Build. Mater*, [e-journal] 23(5), pp.1828-1836. <http://dx.doi.org/10.1016/j.conbuildmat.2008.09.020>.

Gerges, N.N., Issa, C.A. and Fawaz, S.A., 2018. Rubber concrete: Mechanical and dynamical properties. *Case Studies in Construction Materials*, [e-journal] 9, p.184. <http://dx.doi.org/10.1016/j.cscm.2018.e00184>.

- Gesoğlu, M., Güneyisi, E., Khoshnaw, G. and İpek, S., 2014. Investigating properties of pervious concretes containing waste tire rubbers. *Construction and Building Materials*, [e-journal] 63, pp.206-213. <http://dx.doi.org/10.1016/j.conbuildmat.2014.04.046>.
- Grinys, A., Balamurugan, M., Augonis, A. and Ivanauskas, E., 2021. Mechanical Properties and Durability of Rubberized and Glass Powder Modified Rubberized Concrete for Whitetopping Structures. *Materials*, [e-journal] 14, p.2321. <http://dx.doi.org/10.3390/ma14092321>.
- Güneyisi, E., Gesoğlu, M. and Özturan, T., 2004. Properties of rubberized concretes containing silica fume. *Cement and Concrete Research*, [e-journal] 34(12), pp.2309-2317. <http://dx.doi.org/10.1016/j.cemconres.2004.04.005>.
- Gupta, T., Chaudhary, S. and Sharma, R.K., 2014. Assessment of mechanical and durability properties of concrete containing waste rubber tire as fine aggregate. *Construction and Building Materials*, [e-journal] 73, pp.562-574. <http://dx.doi.org/10.1016/j.conbuildmat.2014.09.102>.
- Gupta, T., Chaudhary, S. and Sharma, R.K., 2016. Mechanical and durability properties of waste rubber fiber concrete with and without silica fume. *Journal of Cleaner Production*, [e-journal] 112(1), pp.702-711. <http://dx.doi.org/10.1016/j.jclepro.2015.07.081>.
- Gupta, T., Sharma, R.K. and Chaudhary, S., 2015. Impact resistance of concrete containing waste rubber fiber and silica fume. *International Journal of Impact Engineering*, [e-journal] 83, pp.76-87. <http://dx.doi.org/10.1016/j.ijimpeng.2015.05.002>.
- Hafiz Ahmad, M. and Awang, H., 2012. The effect of steel fibre inclusion on the mechanical properties and durability of lightweight foam concrete. *Advanced Engineering Informatics*.
- Hameed, A.S. and Shashikala, A.P., 2016. Suitability of rubber concrete for railway sleepers. *Perspectives in Science*, [e-journal] 8, pp.32-35. <http://dx.doi.org/10.1016/j.pisc.2016.01.011>.
- Hamouda, H., 2015. Effect of Superplasticizer on Workability of Concrete Containing Crumb Rubber. *Civil and Environmental Research*, 7(2).
- He, L. et al., 2021. Research on the properties of rubber concrete containing surface-modified rubber powders. *Journal of Building Engineering*, [e-journal] 35, p.101991. <http://dx.doi.org/10.1016/j.jobbe.2020.101991>.
- Ismail, M.K. and Hassan, A.A.A., 2016. Use of metakaolin on enhancing the mechanical properties of self-consolidating concrete containing high percentages of crumb rubber. *Journal of Cleaner Production*, [e-journal] 125, pp.282-295. <http://dx.doi.org/10.1016/j.jclepro.2016.03.044>.

Ismail, M.K. and Hassan, A.A.A., 2017. Impact Resistance and Mechanical Properties of Self-Consolidating Rubberized Concrete Reinforced with Steel Fibers. *Journal of Materials in Civil Engineering*, [e-journal] 29(1), p.04016193. [http://dx.doi.org/10.1061/\(asce\)mt.1943-5533.0001731](http://dx.doi.org/10.1061/(asce)mt.1943-5533.0001731).

Kanadasan, J. et al., 2015. Feasibility Studies of Palm Oil Mill Waste Aggregates for the Construction Industry. *Materials (Basel, Switzerland)*, [e-journal] 8(9), pp.6508-6530. <http://dx.doi.org/10.3390/ma8095319>.

Kara De Maeijer, P., Craeye, B., Blom, J. and Bervoets, L., 2021. Rubber in Concrete—The Barriers for Application in the Construction Industry. *Infrastructures*, [e-journal] 6, p.116. <http://dx.doi.org/10.3390/infrastructures6080116>.

Kardos, A.J. and Durham, S.A., 2015. Strength, durability, and environmental properties of concrete utilizing recycled tire particles for pavement applications. *Construction and Building Materials*, [e-journal] 98, pp.832-845. <http://dx.doi.org/10.1016/j.conbuildmat.2015.08.065>.

Kjellsen, K., Wallevik, O. and Fjällberg, L., 1998. Microstructures and microchemistry of the paste-aggregate interfacial transition zone of high-performance concrete. *Advances in Cement Research*, [e-journal] 10(1), pp.33-40. <http://dx.doi.org/10.1680/adcr.1998.10.1.33>.

Kunther, W., Ferreiro, S. and Skibsted, J., 2017. Influence of the Ca/Si Ratio on the Compressive Strength of Cementitious Calcium-Silicate-Hydrate Binders. *Journal of Materials Chemistry A*, [e-journal] 5(33). <http://dx.doi.org/10.1039/C7TA06104H>.

Lee, H. S., Lee, H., Moon, J. S. and Jung, H. W., 1998. Development of Tire Added Latex Concrete. *ACI Materials Journal*, 95(4), pp.356-364.

Li, G., Zhao, X., Rong, C. and Wang, Z., 2010. Properties of polymer modified steel fiber-reinforced cement concretes. *Construction and Building Materials*, [e-journal] 24(7), pp.1201-1206. <http://dx.doi.org/10.1016/j.conbuildmat.2009.12.020>.

Li, L., Ruan, S. and Zeng, L., 2014. Mechanical properties and constitutive equations of concrete containing a low volume of tire rubber particles. *Construction and Building Materials*, [e-journal] 70, pp.291-308. <http://dx.doi.org/10.1016/j.conbuildmat.2014.07.105>.

Ling, T. C., 2011. Prediction of density and compressive strength for rubberized concrete blocks. *Construction and Building Materials*, [e-journal] 25(11), pp.4303-4306. <http://dx.doi.org/10.1016/j.conbuildmat.2011.04.074>.

Ling, T.-C., Nor, H.Md. and Hainin, Mohd.R., 2009. Properties of crumb rubber concrete paving blocks with SBR latex. *Road Materials and Pavement Design*, [e-journal] 10(1), pp.213-222. <http://dx.doi.org/10.1080/14680629.2009.9690188>.

- Liu, R., Li, H., Jiang, Q. and Meng, X., 2020. Experimental investigation on flexural properties of directional steel fiber reinforced rubberized concrete. *Structures*, [e-journal] 27, pp.1660-1669. <http://dx.doi.org/10.1016/j.istruc.2020.08.007>.
- Li, W., Huang, Z., Wang, X. and Zang, Z., 2014. Experimental Study on Proportion of Tensile Strength and Compressive. *Advanced Materials Research*, [e-journal] 919-921, pp.1916-1919. <http://dx.doi.org/10.4028/www.scientific.net/AMR.919-921.1916>.
- Marchment, T., Sanjayan, J. G., Nematollahi, B. and Xia, M., 2019. Interlayer Strength of 3D Printed Concrete: Influencing Factors and Method of Enhancing. In: J. G. Sanjayan, A. Nazari and B. Nematollahi, eds. *3D Concrete Printing Technology*. Butterworth-Heinemann: s.n., pp.241-264. <https://doi.org/10.1016/B978-0-12-815481-6.00012-9>.
- Marie, I., 2016. Zones of weakness of rubberized concrete behavior using the UPV. *Journal of Cleaner Production*, [e-journal] 116, pp.217-222. <http://dx.doi.org/10.1016/j.jclepro.2015.12.096>.
- Mohammed, B. S., Awang, A. B., Wong, S. S. and Nhavene, C. P., 2016. Properties of nano silica modified rubbercrete. *Journal of Cleaner Production*, [e-journal] 119, pp.66-75. <http://dx.doi.org/10.1016/j.jclepro.2016.02.007>.
- Mohsin, A. I. and Fahad, B. M., 2015. Study the Addition of Styrene–Butadiene Rubber Latex on the Workability and Flexural Strength of Crumb Rubber-Mortar. *Chemistry and Materials Research*, 7(6).
- Moustafa, A. and ElGawady, M.A., 2015. Mechanical properties of high strength concrete with scrap tire rubber. *Construction and Building Materials*, [e-journal] 93, pp.249-256. <http://dx.doi.org/10.1016/j.conbuildmat.2015.05.115>.
- Muñoz-Sánchez, B., Arévalo-Caballero, M.J. and Pacheco-Menor, M.C., 2016. Influence of acetic acid and calcium hydroxide treatments of rubber waste on the properties of rubberized mortars. *Materials and Structures*, [e-journal] 50(1), pp.1-16. <http://dx.doi.org/10.1617/s11527-016-0912-7>.
- Ohama, Y., 1995. *Handbook of polymer-modified concrete and mortars: properties and process technology*. s.l.:William Andrew.
- Oikonomou, N. and Mavridou, S., 2009. Improvement of chloride ion penetration resistance in cement mortars modified with rubber from worn automobile tires. *Cement and Concrete Composites*, [e-journal] 31(6), pp.403-407. <http://dx.doi.org/10.1016/j.cemconcomp.2009.04.004>.
- Pelisser, F., Zavarise, N., Longo, T.A. and Bernardin, A.M., 2011. Concrete made with recycled tire rubber: Effect of alkaline activation and silica fume addition. *Journal of Cleaner Production*, [e-journal] 19(6-7), pp.757-763. <http://dx.doi.org/10.1016/j.jclepro.2010.11.014>.

Raj, B., Sathyan, D., Madhavan, M.K. and Raj, A., 2020. Mechanical and durability properties of hybrid fiber reinforced foam concrete. *Construction and Building Materials*, [e-journal] 245, p.118373. <http://dx.doi.org/10.1016/j.conbuildmat.2020.118373>.

Shen, W. et al., 2013. Investigation on polymer–rubber aggregate modified porous concrete.. *Construction and Building Materials*, [e-journal] 38, pp.667-674. <http://dx.doi.org/10.1016/j.conbuildmat.2012.09.006>.

Siddika, A. et al., 2019. Properties and utilizations of waste tire rubber in concrete: A review. *Construction and Building Materials*, [e-journal] 224, pp.711-731. <http://dx.doi.org/10.1016/j.conbuildmat.2019.07.108>.

Siddique, R., 2007. *Waste materials and by-products in concrete*. Heidelberg: Springer Science & Business.

Sienkiewicz, M., Kucinska-Lipka, J., Janik, H. and Balas, A., 2012. Progress in used tyres management in the European Union: A review. *Waste Management*, [e-journal] 32(10), pp.1742-1751. <http://dx.doi.org/10.1016/j.wasman.2012.05.010>.

Soni, E. K. and Joshi, Y., 2014. Performance Analysis of Styrene Butadiene Rubber-Latex on Cement Concrete Mixes. *Journal of Engineering Research and Applications*, 4(3), pp.838-844.

Soroushian, P. and Tlili, A., 1991. Latex modification effects on the impact resistance and toughness of plain and steel-fiber-reinforced concretes. *Transportation Research Record*, 1301, pp.6-11.

Su, H. et al., 2015. Properties of concrete prepared with waste tyre rubber particles of uniform and varying sizes. *Journal of Cleaner Production*, [e-journal] 91, pp.288-296. <http://dx.doi.org/10.1016/j.jclepro.2014.12.022>.

Sukontasukkul, P., Jamnam, S., Rodsin, K. and Banthia, N., 2013. Use of rubberized concrete as a cushion layer in bulletproof fiber reinforced concrete panels. *Construction and Building Materials*, [e-journal] 41, pp.801-811. <http://dx.doi.org/10.1016/j.conbuildmat.2012.12.068>.

Tabassum, N., Biswas, P., Islam, M. and Islam, M., 2018. A Study on the Compressive and Flexural Strength Behavior of Steel Fiber Reinforced Concrete Beam. *International Journal of Advanced Research*, 6(8), pp.557-567.

Tantawi, H. M. Y., 2015. *Introduction to Concrete Technology*, Tabouk: Fahad Bin Sultan University.

Thomas, B.S. and Chandra Gupta, R., 2016. Properties of high strength concrete containing scrap tire rubber. *Journal of Cleaner Production*, [e-journal] 113, pp.86-92. <http://dx.doi.org/10.1016/j.jclepro.2015.11.019>.

- Thomas, B.S., Damare, A. and Gupta, R.C., 2013. Strength and durability characteristics of copper tailing concrete. *Construction and Building Materials*, [e-journal] 48, pp.894-900. <http://dx.doi.org/10.1016/j.conbuildmat.2013.07.075>.
- Thomas, B.S., Gupta, R.C., Kalla, P. and Cseteneyi, L., 2014. Strength, abrasion and permeation characteristics of cement concrete containing discarded rubber fine aggregates. *Construction and Building Materials*, [e-journal] 59, pp.204-212. <http://dx.doi.org/10.1016/j.conbuildmat.2014.01.074>.
- Tomosawa, F., Noguchi, T. and Tamura, M., 2005. The way concrete recycling should be. *Journal of Advanced Concrete Technology*, [e-journal] 3(1), pp.3-16. <http://dx.doi.org/10.3151/jact.3.3>.
- Topçu, İ.B. and Demir, A., 2007. Durability of rubberized mortar and concrete. *Journal of materials in Civil Engineering*, [e-journal] 19(2), pp.173-178. [http://dx.doi.org/10.1061/\(asce\)0899-1561\(2007\)19:2\(173\)](http://dx.doi.org/10.1061/(asce)0899-1561(2007)19:2(173)).
- Topçu, İ.B. and Unverdi, A., 2018. Scrap tires/crumb rubber. In: *Waste and Supplementary Cementitious Materials in Concrete*. s.l.:Woodhead Publishing, pp.51-77.
- Wu, Z., Shi, C., He, W. and Wu, L., 2016. Effects of steel fiber content and shape on mechanical properties of ultra high performance concrete. *Construction and Building Materials*, [e-journal] 103, pp.8-14. <http://dx.doi.org/10.1016/j.conbuildmat.2015.11.028>.
- Xue, J. and Shinozuka, M., 2013. Rubberized concrete: A green structural material with enhanced energy-dissipation capability. *Construction and Building Materials*, [e-journal] 42, pp.196-204. <http://dx.doi.org/10.1016/j.conbuildmat.2013.01.005>.
- Xu, F., Zhou, M., Chen, J. and Ruan, S., 2014. Mechanical performance evaluation of polyester fiber and SBR latex compound-modified cement concrete road overlay material. *Construction and Building Materials*, [e-journal] 63, pp.142-149. <http://dx.doi.org/10.1016/j.conbuildmat.2014.04.054>.
- Xu, J., Yao, Z., Yang, G. and Han, Q., 2020. Research on crumb rubber concrete: From a multi-scale review. *Construction and Building Materials*, [e-journal] 232, p.117282. <http://dx.doi.org/10.1016/j.conbuildmat.2019.117282>.
- YTL Cement, 2022. *Cement (Bag)*. [online] Available at: <https://ytlcement.my/cement-bag/> [Accessed 21 August 2022].

APPENDICES

Appendix A

Appendix A-1: Sieve Analysis of Coarse Aggregate.

Sieve Size (mm)	Weight (g)			Culmulative Percentage (%)		
	Empty Sieve	Aggregate retained + sieve	Aggregate retained on each sieve	Aggregate retained on each sieve (%)	Coarser	Finer
25	394.6	394.6	0	0	0	100
20	391.0	391.0	0	0	0	100
14	397.4	847.2	449.8	44.98	44.98	55.02
10	445.8	696.8	251.0	25.1	70.08	29.92
5	474.6	682.4	207.8	20.78	90.86	9.14
4.75	240.0	331.4	91.4	9.14	100	0
Total			1000	100		

Appendix B-2: Sieve Analysis of Fine Aggregate.

Sieve Size (mm)	Weight (g)			Culmulative Percentage (%)		
	Empty Sieve	Aggregate retained + sieve	Aggregate retained on each sieve	Aggregate retained on each sieve (%)	Coarser	Finer
4.75	489.2	496.4	7.2	1.44	1.44	100
2.40	467.8	481.0	13.2	2.64	4.08	97.36
1.20	467.0	546.6	79.6	15.92	20	81.44
0.60	334.6	427.4	92.8	18.56	38.56	62.88
0.30	340.6	476.0	135.4	27.08	65.64	35.8
0.15	333.4	444.6	111.2	22.24	87.88	13.56
0.063	244.8	305.4	60.6	12.12	100	1.44
Total			500	100		

Appendix C-3: Sieve Analysis of Crumb Rubber.

Sieve Size (mm)	Weight (g)			Culmulative Percentage (%)		
	Empty Sieve	Aggregate retained + sieve	Aggregate retained on each sieve	Aggregate retained on each sieve (%)	Coarser	Finer
4.75	489.2	489.6	0.4	0.08	0.08	100
2.40	468.4	790.0	321.6	64.32	64.4	35.68
1.20	467.6	635.2	167.6	33.52	97.92	2.16
0.60	334.8	345.0	10.2	2.04	99.96	0.12
0.30	341.0	341.2	0.2	0.04	100	0.08
0.15	334.2	334.2	0	0	100	0.08
0.063	244.8	244.8	0	0	100	0.08
Total			500	100		

Appendix D-4: Compressive Strength for Trial Mixes of LRC-CTR.

W/C Ratio	Compressive Strength (MPa)					
	7 days			28 days		
	1	2	3	1	2	3
0.28	53.28	51.78	52.26	55.83	55.77	58.25
0.30	42.62	45.32	-	45.61	54.63	45.45
0.32	36.28	38.66	38.73	37.77	45.21	32.09

Appendix E-5: Compressive Strength for Trial Mixes of LRC-15 % SF.

W/C Ratio	Compressive Strength (MPa)					
	7 days			28 days		
	1	2	3	1	2	3
0.28	55.73	54.81	56.75	59.18	60.61	62.89
0.30	51.03	51.73	51.45	57.97	60.72	59.71
0.32	35.14	46.37	44.72	54.79	53.44	53.64

Appendix F-6: Compressive Strength of LRC-CTR and LRC-15 % SF.

Curing Period (days)	Compressive Strength (MPa)					
	LRC-CTR			LRC-15 % SF		
	1	2	3	1	2	3
7	52.22	52.62	53.82	58.44	56.79	-
28	63.11	60.82	62.55	65.65	65.35	-
56	64.86	68.96	59.46	66.37	68.04	65.02

Appendix G-7: Splitting Tensile Strength of LRC-CTR and LRC-15 % SF.

Curing Period (days)	Splitting Tensile Strength (MPa)					
	LRC-CTR			LRC-15 % SF		
	1	2	3	1	2	3
7	15.73	11.13	10.46	12.27	15.45	16.62
28	13.05	15.76	14.90	17.96	16.88	16.25
56	18.26	18.02	19.83	21.02	18.02	23.06

Appendix H-8: Flexural Strength of LRC-CTR and LRC-15 % SF.

Curing Period (days)	Flexural Strength (MPa)					
	LRC-CTR			LRC-15 % SF		
	1	2	3	1	2	3
7	5.57	5.47	5.49	6.39	6.58	6.24
28	6.20	5.24	5.25	6.31	7.30	7.13
56	5.77	5.96	6.33	6.81	7.37	7.12